Svoluji k zapůjčení své diplomové práce ke studijním účelům a prosím, aby byla vedena přesná evidence vypůjčovatelů. Převzaté údaje je vypůjčovatel povinen řádně ocitovat.

Univerzita Karlova
Přírodovědecká fakulta

Studijní program: Biologie
Studijní obor: Genetika, molekulární biologie a virologie

Bc. Zuzana Kružíková

Příprava nanočástic pro terapii viru žloutenky typu B

Preparation of nanoparticles for hepatitis B viral therapy

Diplomová práce

Vedoucí práce/Školitel:
Mgr. Klára Grantz Šašková, Ph.D.

Praha, 2018

Prohlašuji, že jsem závěrečnou práci zpracovala samostatně a že jsem uvedla všechny použité informační zdroje a literaturu. Tato práce ani její podstatná část nebyla předložena k získání jiného nebo stejného akademického titulu.

V Praze, 27. 4. 2018

Bc. Zuzana Kružíková

Velice děkuji své školitelce Kláře Grantz Šaškové za její ochotnou pomoc, podporu a předané nadšení z výzkumu. Za pomoc a výborný kolektiv děkuji i ostatním jejím studentům a všem členům laboratoře Jana Konvalinky, kde máme to štěstí náš výzkum realizovat, zejména Janě Starkové, Michalu Svobodovi, Františku Sedlákovi a Janu Belzovi. Dále děkuji Petru Cíglerovi a jeho skupině za pomoc s chemickou částí projektu a spolupráci při sestavování a charakterizaci nanočástic, jmenovitě Václavu Vaňkovi, Jitce Neburkové a Janu Vávrovi. Děkuji i Janu Weberovi za možnost posunout náš projekt dál a zapojit se do jeho týmu ve virologické BSL3 laboratoři, z nějž patří mé díky především Barboře Lubyové a Janu Hodkovi.

Abstrakt

Virus hepatitidy B (HBV) je v současné době cílem zájmů na poli základního i farmaceutického výzkumu. Účinná vakcína proti HBV byla vyvinuta již v roce 1982, přesto je však světová prevalence tohoto onemocnění stále vysoká. Chronická infekce HBV může vést k významnému poškození jater a postupně až ke vzniku hepatocelulárního karcinomu. Pro chronickou infekci ovšem stále neexistuje vhodná léčba, jelikož virový genom zůstává v jádře infikovaného hepatocytu ukryt imunitnímu systému ale i antivirovým léčivům. Jedna z nových strategií pro léčbu HBV předpokládá, že virová cccDNA by mohla být zničena pomocí nástrojů genové editace jako je CRISPR/Cas9 systém. Aby mohl být tento systém pro genovou editaci uveden do klinické praxe, CRISPR/Cas9 musí být specificky dopraven do cílových buněk, aby se minimalizovalo riziko štěpení DNA mimo cílené sekvence. Tato diplomové práce se zabývá zaprvé návrhem nových sgRNA mířených proti cccDNA viru hepatitidy B a testování jejich účinnosti a zadruhé tato práce popisuje modulární lipidové nanočástice vyvinuté speciálně pro dopravu CRISPR/Cas9 ve formě RNA.

Klíčová slova: virus hepatitidy B, CRISPR/Cas9, editace genů, lipidové nanočástice, dopravování mRNA, cílené dopravování

Abstract

Hepatitis B virus (HBV) represents one of the hot topics of current basic and pharmaceutical research. Although an effective vaccine against HBV exists since 1982, the world prevalence of chronic infection is still alarming. The infection can lead to significant liver damage, often resulting in hepatocellular carcinoma. Chronic HBV infection cannot be cured due to the fact that the viral genome persists in the infected hepatocyte hidden from the host immune response as well as from the antiviral treatment. One of the novel approaches aiming for HBV cure suggests that this cccDNA pool could be destroyed using gene editing tools such as CRISPR/Cas9 system. In order to shift this gene editing system to possible medicinal application, CRISPR/Cas9 has to be specifically delivered into the target cell in order to minimize its putative off-target activity. This thesis focuses at first on the design and efficacy testing of new sgRNAs targeting HBV cccDNA and secondly, it describes modular lipid nanoparticles developed specially for delivery of the CRISPR/Cas9 system in the form of RNA.

Keywords: hepatitis B virus, CRISPR/Cas9, gene editing, lipid nanoparticles, mRNA delivery, targeted delivery

List of abbreviations

HBV	hepatitis B virus
ASGPR	asialoglycoprotein receptor
Cas9	CRISPR-associated protein 9
cccDNA	covalently closed circular DNA
CRISPR	clustered regularly interspaced short palindromic repeats
CTL	cytotoxic T lymphocyte
DMG	diacylglycerol
DOPE	1,2-dioleyol-sn-glycero-3-phosphoethanolamine
DSB	double strand break
HBeAg	hepatitis B core antigen
HBsAg	hepatitis B surface antigen
HDR	homology directed repair
LNP	lipid nanoparticle
NHEJ	non-homologous end joining
NTCP	Na-taurocholate cotransporting polypeptide receptor
PAGE	polyacrylamide gel electrophoresis
PAM	protospacer adjacent motif
PCR	polymerase chain reaction
PEG	poly(ethylene) glycol
pgRNA	pregenomic RNA
rcccDNA	recombinant cccDNA
rcDNA	relaxed circular DNA
sgRNA	single guide RNA

TALEN	transcription activator-like effector nuclease
Tf	transferrin
TT3	N^1,N^3,N^5-tris(2-aminoethyl)benzene-1,3,5-tricarbomide
ZFN	zinc finger nuclease

Contents

1. Introduction

Hepatitis B virus (HBV) has been extensively studied over the past 50 years. It causes a potentially life-threatening liver infection and although the effective vaccine is available from 1982, it still represents a global health problem. According to the data from the World Health Organization, there are about 257 million people infected worldwide, of which many suffer from chronic hepatitis. That, for instance, resulted in 887 000 deaths in the year 2015, mostly due to HBV-associated liver cirrhosis and hepatocellular carcinoma. In some African regions, the HBV prevalence is as high as 6.2 % of adults (WHO 2017) and the biggest problem represents a mother-child transmission putting thus the child on a high risk of the development of chronic hepatitis.

Hepatitis B virus can be transmitted through contact with blood or other body fluids of an infected person. At first, it causes an acute infection that is usually asymptomatic. The major problem of HBV infection starts with its potential progress into the chronic stadium which can cause irreversible liver damage represented by liver cirrhosis, fibrosis or hepatocellular carcinoma. The current treatment by antiviral agents focusses on the chronic phase and usually lowers the risk of HBV-associated liver damage. However, the viral genome (cccDNA, see further) stays hidden to current antiviral therapy, maintains in the nucleus of an infected cell and thus makes the ultimate cure currently impossible. Several approaches aiming at this so called HBV latent phase have been tested including those exploiting the gene editing tools.

The research of gene editing experienced a revolution in the past five years with the development of the CRISPR/Cas9 system. This system can target specific DNA sequences and enable their editing with a minimal off-site activity. Several studies have been published using this approach to mutate or degrade the HBV minichromosome, some of them with encouraging outcome. Although the idea of using the CRISPR/Cas9 for HBV cccDNA degradation seems very promising, several issues have to be solved including off-target exclusion and specific and stable delivery.

As mentioned above, an important part of introducing this concept for potential applications involves the delivery of this system into the infected cells. It is necessary to find a system that would be well-tolerated by the cell without causing any damage. The goal is to develop non-cytotoxic, non-immunogenic and biodegradable nanoparticles that could be specifically targeted into infected hepatocytes. Inspired by a natural cell membrane, liposomes have been already utilized to deliver various cargos into the cells. Some of the liposomal

systems include artificial lipids that have been incorporated into their structure to improve their biophysical and biological properties and modularity - an easy addition of a small molecule interacting with specific cell receptor (in our case a hepatocyte receptor) could bring a great benefit enabling specific cell delivery.

The project described in this thesis focuses first on the design of the specific CRISPR/Cas9 system for degradation of the HBV cccDNA molecule in an infected cell and secondly on the development of a liposome-based modular delivery system of the CRISPR/Cas9 enabling targeting into the hepatocytes.

2. Literature Review

2.1. Hepatitis B virus

Hepatitis B virus is a DNA virus which belongs to the *Hepadnaviridae* family. It is a small enveloped virus of size about 42 nm with icosahedral core. The viral genome is presented in an infectious virion as a partially double-stranded DNA molecule in relaxed circular conformation with a small overhang and covalently bound DNA polymerase. The genome consists of about 3200 bases and it encodes surface and core proteins (with their longer versions PreS1, PreS2, and PreCore) as well as viral polymerase and X protein (Fig. 1A). The genome also contains two enhancers both with a specific function in hepatocytes. The first DNA strand is almost a complete circle, it is referred as a "minus" strand while the second incomplete strand has a variable length with a gap of 600 – 1200 nucleotides (Lau & Wright, 1993; Summers *et al.*, 1975).

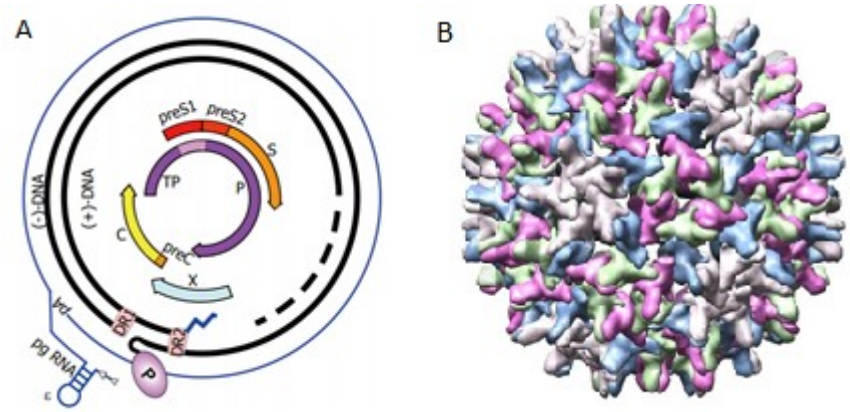

Fig. 1. **Hepatitis B viral genome organization and the 3D structure of the viral capsid**. **A)** HBV DNA genome consists of one almost complete (-) strand with an overhang including a covalently bound polymerase to the 5' end, and a second incomplete (+) strand of variable length. Viral proteins are indicated with respect to the relative locations of encoding regions. Pregenomic RNA with the 5' hairpin structure that serves as a template for viral DNA polymerase is depicted in blue (adapted from (Beck & Nassal, 2007). **B)** Crystal structure of the viral capsid solved at 3.3 Å resolution by X-ray (PDB 1QGT (Wynne *et al.*, 1999).

The virus is composed of an outer envelope derived from the host lipid membrane containing the HBV surface proteins, and an inner icosahedral protein capsid that contains the genomic DNA (nucleocapsid) and a DNA polymerase with a reverse transcriptase activity similar to retroviruses. The capsid is composed of a single polypeptide chain of a molecular weight of 20 kDa, also known as the core antigen, HBcAg (Fig. 1B). There are also

pleomorphic forms of various shapes lacking the inner capsid. These "bodies" are non-infectious and are composed mostly of lipid and the surface antigen (HBsAg) that is excessively expressed over the viral life cycle.

Even though HBV is a DNA virus, it uses an RNA intermediate during its life cycle which is the cause of genetic instability and high mutagenic rate. There are ten different genotypes (known as A – J) and we distinguish four main serotypes (ayw, ayr, adw, adr) based on antigenic epitopes presented on the envelope proteins. Regarding geographical distribution, they are not equally spread – while genotypes A and D are mostly found in the US and Europe, genotypes B and C appear mainly in China and Southeast Asia (Grimm *et al.*, 2011).

There are several types of HBV infecting other species than humans. An important example is the duck hepatitis B virus that often serves as a research model even though it has a shorter genome compared to HBV infecting humans and does not contain any X protein (Schultz *et al.*, 1999). The HBV can be also transmitted to great apes such as orangutan and chimpanzee (Warren *et al.*, 1999; Zuckerman *et al.*, 1978). Moreover, it was reported that the HBV can also infect macaques that could serve as an excellent nonhuman primate research model (Dupinay *et al.*, 2013).

2.1.1. HBV life cycle

The life cycle of *Hepadnaviridae* family has been studied in detail during the past fifty years with the understandable emphasis on the human HBV. The human HBV recognizes the NTCP receptor expressed on the surface of liver cells (Yan *et al.*, 2012). After viral binding to the NTCP, it enters the cell via receptor mediated endocytosis (Fig. 2). Once inside the cell, the viral capsid is uncoated and transported into the cell nucleus where the viral genome is released. The DNA genome is, at this moment, in a form of rcDNA (relaxed circle) consisting of one complete (-) and second incomplete (+) DNA strand with DNA polymerase covalently bound on the first (-) strand (Seeger & Mason, 2015).

In a nucleus, the stalled polymerase is recognized by the host endogenous DNA repair mechanisms. The viral polymerase is cut off, the incomplete strand is repaired and the viral DNA forms the so called cccDNA (covalently closed circular DNA) (Fig. 2). The cccDNA interacts with histone and other non-histone proteins and forms a nucleosome and a minichromosome structure. HBV core protein was also shown to interact with HBV cccDNA and is involved in reducing the nucleosomal spacing of the viral DNA (Bock *et al.*, 2001).

Another regulator of cccDNA is protein X (HBx) that was reported to participate in transcription regulation. HBx recruits the cellular histone acetyltransferases, whereas histone deacetylases are recruited in the absence of HBx (Belloni *et al.*, 2009). Various host regulation factors can bind to promoters or other sites of HBV cccDNA leading to transcription activation and nucleosome mobility (Tropberger *et al.*, 2015). The overall process of cccDNA transcription still remains to be uncovered and is currently heavily studied in the HBV field.

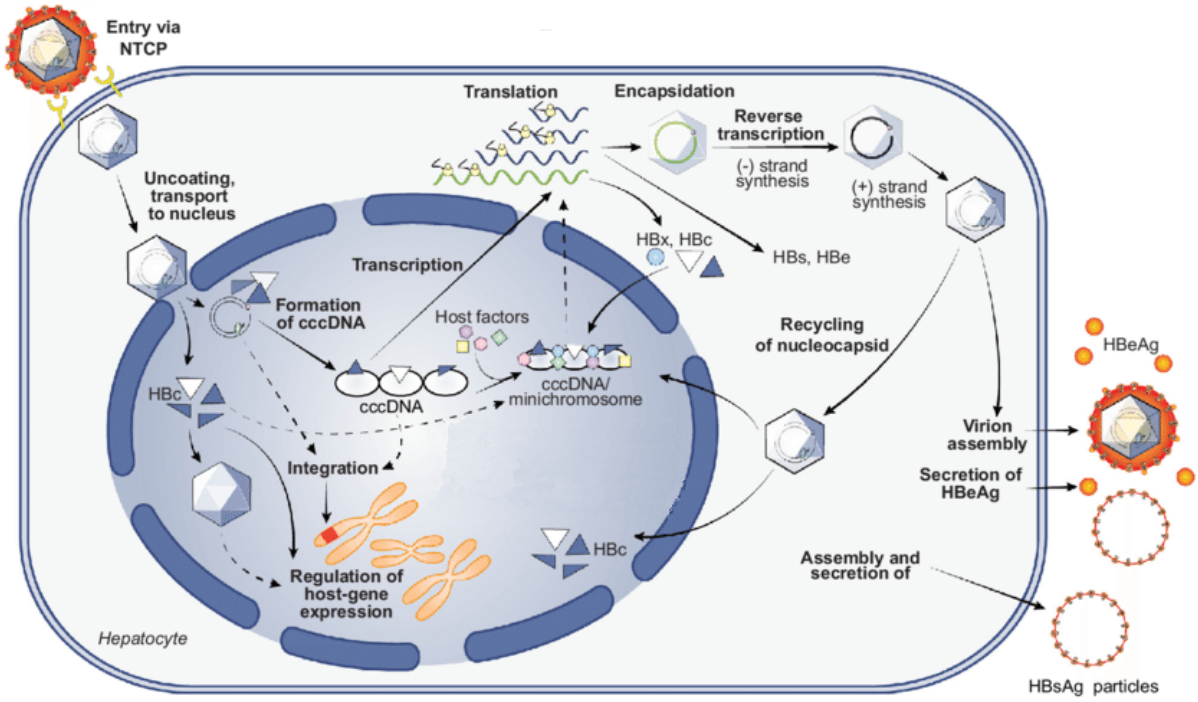

Fig. 2. **HBV life cycle.** HBV enters the hepatocytes via the NTCP receptor. The viral capsid is uncoated inside the cell and the viral genome is transported into the nucleus where the cccDNA is formed. The HBV genome stays as a minichromosome interacting with several regulatory proteins like HBx, HBc or various host factors or it can be potentially integrated into the host chromosomes. New viral capsids containing pgRNA are assembled in the cytoplasm. pgRNA is reversely transcribed into the DNA (-) strand. After synthesis of (+) strand, the capsid is transported back into the nucleus or it is secreted with an envelope derived from the cell membrane and viral surface protein. Moreover, empty particles consisting of surface proteins are secreted in order to distract the immune system (adapted from (Durantel & Zoulim, 2016).

Cellular RNA polymerase II is used for transcription of the viral DNA into RNA. Together with transcription and translation of viral proteins, pgRNA (pregenomic RNA) is transcribed and translocated into the cytoplasm where the new viral capsid is assembled. During maturation of the capsid, pgRNA is reversely transcribed into the DNA by viral RNA dependent DNA polymerase which is encapsulated together with the pgRNA. Some of the

new capsids return to the nucleus to maintain the infection level inside the particular cell while the rest of the capsids are released from the cells to infect other hepatocytes (Fig. 2). Apart from 42 nm infectious viral particles, there are also 22 nm rods and spheres assembled from surface proteins and released into the blood. They are called Dane particles, they are much more abundant than the whole infectious particles and their main function is to distract the immune system in advantage of viral particles containing HBV genome which can thus escape the immune response (Beck & Nassal, 2007; Grimm *et al.*, 2011).

Reverse transcription is an essential step in a life cycle of retroviruses. Unlike HBV, which is a DNA virus, an infectious particle of retrovirus contains a genome in a form of RNA. Another important difference is that retroviruses integrate their DNA into the host chromosomes after the reverse transcription of RNA inside the cell. Normally, cccDNA of the HBV remains as an individual chromosome-like molecule. However, it has been reported that in some cases HBV DNA is also integrated into the host chromosomes (Fig. 2). HBV does not contain its own integrase like retroviruses, thus the integration is rather an accident made by the host cell. It has been proven that the HBV DNA is integrated into a host DNA mostly at damaged sites. The viral DNA is probably joined by nonhomologous end joining and, once integrated, it can later cause changes in DNA sequence or structure (Bill & Summers, 2004). The differences between episomal and integrated forms of HBV DNA may also present alterations in the potential development of the disease, treatment or even possibility of a cure.

2.1.2. Hepatitis B infection

After the infection, the virus is quickly spread through the whole liver and the next fate of the patient depends on his or her immune response. About 90 % of adults do not develop any apparent symptoms. HBV infection itself is non-cytopathic. Histopathology of the liver is a consequence of cytotoxic T lymphocyte (CTL) effects and other adaptive immune reactions. There is a rare risk of fulminant hepatitis when the immune response is so strong that the CTLs destroy basically the whole liver which leads to the death of the patient. In the remaining 10 % of adults and reversely in 90 % of children (mostly under 1-year-old, children often infected from their mothers) infected with hepatitis B virus, the transient infection is not cleared because of ineffective immune response and it becomes chronic (Seeger & Mason, 2015).

It was shown that the replication of HBV starts already one hour after infection. Shortly after that, levels of interferon gamma and interleukin 12 are increasing. Later, NK cells are

activated and start reducing the infection. The innate immune response lasts a few days, whereas the T cells are detectable several weeks from the infection. The immune system must avoid high levels of inflammation and necrosis in the liver tissue to prevent irreversible damage. It was reported that after the cell division, HBV survives and remains in the newly formed cells (Dandri *et al.*, 2000). Therefore, fast and efficient immune response is necessary to prevent the development of chronic hepatitis (Guy *et al.*, 2008).

In 2014 a concept of cccDNA clearance was proposed: interferon-alfa and lymphotoxin-beta receptor together recruit the APOBEC3A and APOBEC3B cytidine deaminase which targets the cccDNA and enables depurination leading to degradation of the whole cccDNA molecule. This concept claims that the infection clearance is independent of cytotoxic reactions and it is intermediated by interferon (Lucifora *et al.*, 2014). Consistently, early studies claimed that interferon-alfa reduces the level of HBV replication. In a duck model, it seemed that the interferon interacts with the HBV core protein which has the main role in the reduction of cccDNA levels. Other results indicated the opposite effect in humans, where the interferon was effective in the absence of the core protein, however, the mechanism or any details were not shown and the effects were not strong enough to clear the whole infection (Schultz *et al.*, 1999). There are many contradictory opinions regarding cccDNA clearance. One hypothesis suggested that the immune system destroys specifically the viral cccDNA molecule without any significant damage to liver, on the other hand, it was suggested that during the immune response leading to resolution of the disease, large amount of hepatocytes infected with HBV is destroyed, however, the old population is replaced by survived hepatocytes so the liver is recovered and repopulated by the new hepatocytes from cell division (Summers *et al.*, 2003).

Chronic hepatitis is a term for infection which lasts for more than six months. Patient virus titers can decline with time but later they rebound with symptoms of acute hepatitis. This can lead to significant liver damage which results in cirrhosis and fibrosis while the risk of subsequent complications is dependent on the virus titer (C. J. Chen & Yang, 2011). Another important problem of chronic hepatitis is the consequent development of hepatocellular carcinoma. It is still not clear what is the main cause of it and if some of the viral proteins can influence the initiation of hepatocyte transformation. It is speculated that cells containing the viral genome can escape the CTL, and in order to repopulate the damaged liver, they undergo multiple cell division during which they are susceptible to mutagenesis and transformation. It is also possible that after the massive destruction by CTL, the liver cells

(without the virus) are genetically or epigenetically modified to proliferate faster so that they prevent the destruction of the whole liver (Seeger & Mason, 2015).

2.1.3. HBV treatment

Although the effective vaccine is available since 1982, more than 257 million people are chronically infected and there is no appropriate method how to eliminate the infection from these individuals. The first-line treatment of chronic HBV infection represents the pegylated interferon-alfa (peginterferon) that has immunomodulatory as well as viral inhibitory properties. It has a high likelihood of hepatitis B surface antigen (HBsAg) clearance and also the absence of drug resistance. The interferon therapy is, however, very burdensome for patients with multiple negative side effects and cannot be used for a long-term treatment. Very effective are nucleotide or nucleoside analogues targeting viral reverse transcriptase – tenofovir and entecavir, respectively. They are the most potent drugs, rarely lead to drug resistance, have only a few side effects and can be taken once a day. Overall, the current treatment can slow the progression of cirrhosis, reduce the incidence of liver cancer and improve long-term survival. Still, it does not lead to HBV total eradication and needs to be continued indefinitely for prevention of viral rebound (Shih *et al.*, 2016). Therefore, a treatment that would lead to HBV cure is urgently needed and represents one of the unmet medical needs. Alternative therapeutic strategies that could be possibly used in combination with current treatment are under investigation.

One of them represents the blockage of the very first step of the viral life cycle - the viral entry into the cell that prevents the spreading of the infection. There are two main substances already under experimental investigation in the treatment of hepatitis B. First of them is a lipopeptide Myrcludex-B, which has been proven to block the infection *de novo* and also blocks the intrahepatic spread post infection (Volz *et al.*, 2013). Second is Cyclosporin A which inhibits the transporter activity of NTCP receptor and thus also blocks the HBV entry (Watashi *et al.*, 2014).

Alternative strategy currently under investigation is to use regulatory siRNA or miRNA. By using siRNA it is possible to knock down the synthesis of viral proteins as well as to block the transcription of new pgRNA necessary for further HBV spread. Experiments with siRNA in transgenic mice showed that the model system works without induction of cytokines and immune response (Wooddell *et al.*, 2013). Furthermore, miRNA was proven to inhibit HBV

replication by targeting two metabolic regulators – namely, it is the miRNA-130a targeting host factors PGC1α and PPARγ ((Huang *et al.*, 2015).

Yet another possibility is represented by the inhibition of capsid formation. Small derivative molecules, that can cause dysregulations in capsid assembly, are already in preclinical trials (Zeisel *et al.*, 2015). Moreover, inhibitors of glycosylation at the endoplasmatic reticulum can be possibly used as inhibitors of virion release (Simsek *et al.*, 2006). Further, inhibitors of endosomal sorting for multivesicular bodies, that are used by HBV, are being investigated (Hurley, 2015), or tetherin which blocks the release of several other enveloped viruses (Evans *et al.*, 2010). Other suggested strategies include epigenetic control of cccDNA and, quite importantly, using of immunotherapy (Shih *et al.*, 2016).

Nevertheless, even with the best efforts to stop the infection spreading between liver cells, blocking the virion release, entry or another part of the viral life cycle, the main hurdle is represented by the HBV cccDNA that stays inside the infected cell, unaffected by the current treatment. HBV cccDNA forms a minichromosome and it thus cannot be easily distinguished from the host DNA. Therefore, to eliminate the HBV infection completely, it is necessary to eliminate this cccDNA pool. The cccDNA destruction thus seems as the only method how the HBV infection could be cured. One way how to achieve that is represented by immunotherapy and the second one, that is further described and investigated in this thesis, uses the state-of-the-art gene editing tools.

2.2. Gene editing tools

The modern history of specific gene editing dates back to 1996 when Dr. Chandrasegaran with his group created zinc finger nuclease (ZFN). They used a DNA-binding motif called zinc finger which is often used by eukaryotic cells. It was first found in transcription factor IIIA of *Xenopus laevis* as a domain binding DNA with zinc ion (J. Miller *et al.*, 1985). The ability of zinc fingers to bind specific DNA sequences seemed promising when combined with a restriction endonuclease that could generate double-strand breaks (DSB). Therefore, this DNA binding motif was linked to the cleavage domain of FokI typeII and the whole protein was dimerized since FokI works as a dimer. The first programmed endonuclease was ready to produce specific gene knockouts (Kim *et al.* 1996). However, many disadvantages of ZFN were later revealed like their time-consuming preparation and mainly their off-targets activities. Even with numerous studies trying to improve ZFN target

specificity, the risk of off-targets was not completely eliminated and thus they are not suitable for therapeutic purposes (Pattanayak *et al.*, 2011).

Furthermore, there were attempts to improve the specificity of programmed nucleases by using different DNA-binding motif. In 2009, transcription activator-like effectors (TALEs) were found in gram-negative bacteria *Xanthomonas*. These bacterial proteins contain a nuclear localization signal so they are translocated into the nucleus after they are injected into a plant cell and they activate transcription by transcription activating domain. TALEs also contain several tandem repeats which together with the amino acid sequence determine the nuclease specific activity (Boch *et al.*, 2009). TALE nucleases (TALENs) were further prepared by fusion of TALEs with the catalytic domain of FokI endonuclease dimer (J. C. Miller *et al.*, 2011). TALENs proved to be more specific and efficient in gene editing than ZFNs. They are more easily prepared and unlike ZFNs they can be designed to target any DNA sequence without any limitations. However, in comparison to ZFN gene of size about 1 kbp, TALEN gene of 3 kbp is much bigger which presents an obstacle in means of their delivery into the cells (Gupta & Musunuru, 2014). After 4 years of extensive work on the TALENs, a system much more effective was found in 2013 that is called CRISPR/Cas9.

2.2.1. CRISPR/Cas9 system

CRISPRs – clustered regularly interspaced short palindromic repeats – were originally found much earlier. They were discovered during analysis of *Iap* gene in *Escherichia coli* where a sequence of five directed homologous repeats of 29 nucleotides interspaced by 32 unique nucleotides was identified (Ishino *et al.*, 1987). However, the function of CRISPRs remained unclear for many years.

From the study performed on *Streptococcus thermofilus*, it was shown that CRISPRs together with CRISPR-associated proteins (Cas proteins) have a role in bacterial adaptive immunity providing a resistance against bacteriophage infection. After the first infection of a bacterium with a particular phage, a new spacer between the CRISPR sequences is integrated from the genome sequence of the infecting phage. During the next infection with the same phage, its DNA sequence is recognized according to this spacer and cleaved by the Cas protein which saves the bacterium from the infection (Barrangou *et al.*, 2007). CRISPRs are present in many Bacteria and Archaea species so the next goal was to prove this concept to be effective in other organisms. CRISPR/Cas system from *S. thermophilus* was transferred into the *Escherichia coli* where it also provided specific resistance against phage infection. After

deeper analysis, proto-spacer adjacent motif (PAM) was identified in the bacteriophage sequence just next to the sequence corresponding to bacterial CRISPR spacer. From all the CRISPR-associated proteins, Cas9 protein (consisting of MrcA/HNH-nuclease and RuvC/RNaseH-like nuclease motif) is able to efficiently cleave the phage genome and stop the infection (Sapranauskas *et al.*, 2011).

Analysis of human pathogen *Streptococcus pyogenes* further revealed the mechanism of phage DNA recognition and cleavage. From the CRISPR locus, trans-activating CRISPR RNA (tracrRNA) is transcribed. This tracrRNA is partially complementary with pre-crRNA – precursor of the CRISPR RNA (crRNA) targeting the phage. These results suggest that tracrRNA binds to the pre-crRNA and enables its maturation in crRNA which is then able to target the Cas9 nuclease to complementary phage DNA sequence (Deltcheva *et al.*, 2011).

The huge potential of engineered CRISPR/Cas9 adapted for research and possibly even therapeutic purposes became obvious and several scientific groups around the world started working on it. It was shown that tracrRNA and crRNA can be synthesized as one molecule – sgRNA (single guide) and it can be designed to target any DNA sequence (Jinek *et al.*, 2012). The only limiting criterion is that the DNA sequence which is to be targeted must be followed by trinucleotide PAM (Gasiunas *et al.*, 2012). Even though the system origins from bacteria it was proven to work efficiently in human and other mammalian cells (Mali *et al.*, 2013).

Cas9 cleavage of DNA (as well as ZFN and TALEN cleavage) produces double-strand breaks (DSB) in the DNA molecule. The cell has two different mechanisms how to repair DSB – it is either non-homologous end joining (NHEJ) or homology-directed repair (HDR) (Fig. 3). HDR is based on homologous recombination (usually of the second chromosome or the second chromatid during mitosis or in case of gene editing, it can be any DNA sequence which is framed by sequences homologous to sequences close to DSB). HDR is common in yeast while in more complexed organisms it is not easy to “find” the homologous chromosome so the DSB are usually repaired by simple NHEJ. NHEJ is fast and efficient so it can save the cell from replication fork stalling or even cell death but it is error-prone and it can be a source of mutagenesis like insertions or deletions (Santiago *et al.*, 2008; Sonoda *et al.*, 2006).

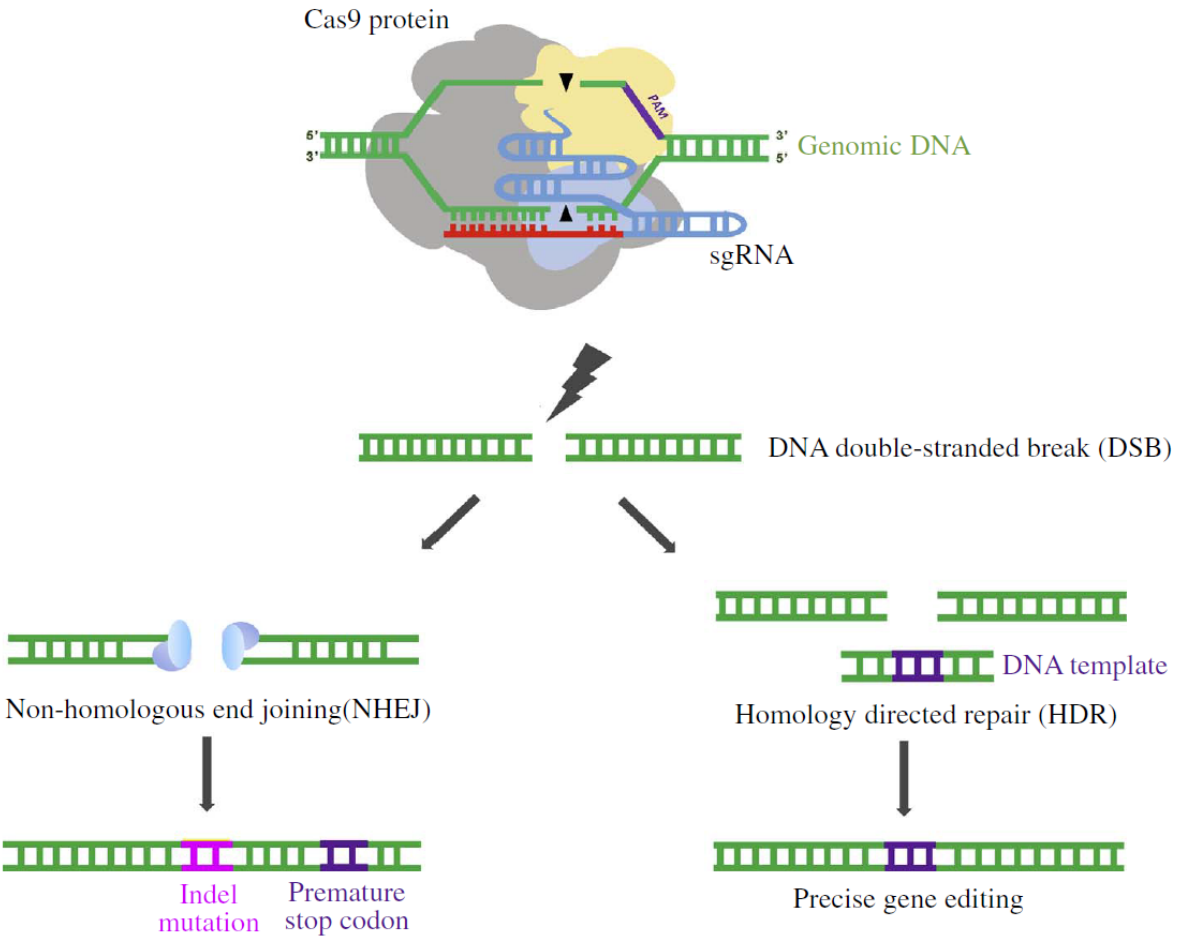

Fig. 3. **Illustration of the CRISPR/Cas9 cleavage and subsequent DNA repair mechanisms**. Complementary sgRNA binds to the DNA and recruits the Cas9 nuclease. DSB resulting from various causes including Cas9 cleavage is repaired *in vivo* by error-prone NHEJ or by precise HDR if the homologous sequence is present (adapted from (C. Liu *et al.*, 2017).

2.2.2. CRISPR/Cas9 targeting HBV

CRISPR/Cas9 system proved as a great gene editing tool for many scientific purposes (i.e. generation of various knock out animals) and opened up a new era of gene editing in clinical therapy. Even though one can imagine using this system for numerous human targets involved in genetic diseases, there are still limitations represented mainly by ethical issues and safety. Using CRISPR/Cas9 targeting HBV cccDNA in order to degrade it seems quite promising, especially because it could lead to HBV cure. Still, the system has to be effective, specific and with minimal (ideally none) off-target activity.

After the cleavage of mammalian chromosomal DNA by the CRISPR/Cas9, double strand breaks are generated that are later repaired by the DNA repair mechanisms such as HDR or NHEJ as mentioned above. It was not obvious, however, if the DNA repair mechanisms would repair cleaved cccDNA established from the virus. Later it was shown that DNA repair in this case works in a similar manner leading to mutagenesis of the cccDNA caused by NHEJ (Seeger & Sohn, 2014). It was further suggested that if the cccDNA is hit multiple times with sgRNAs targeting different sites within the HBV genome, a large segment of DNA could be removed. This could lead to total degradation of the HBV cccDNA or at least it could cause significant alterations of the HBV genome that would disable expression of the functional virus. This could ultimately lead to HBV cure (Fig. 4).

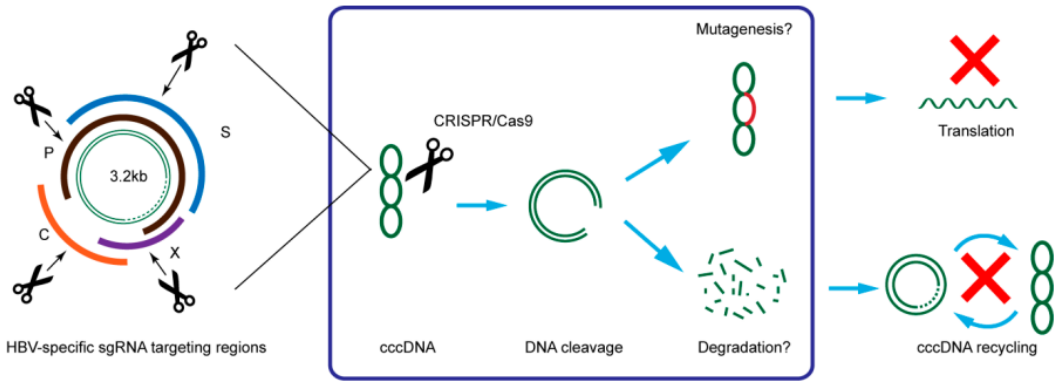

Fig. 4. **Targeting CRISPR/Cas9 against HBV**. Cas9 cleavage enabled by sgRNA targeting one or more regions of HBV genome can result in significant mutagenesis blocking translation of viral proteins or potentially in degradation of the whole viral cccDNA (Adapted from (G. Lin *et al.*, 2015).

The whole concept was later proven to be correct. It was shown that CRISPR/Cas9 decreases the viral DNA levels by 100 to 1000 folds after transduction of the cell in a lentiviral vector. Sequence analysis of the viral DNAs left in the cell revealed insertion or deletions within the targeted sequences. The mutagenesis caused by CRISPR/Cas9 system was sufficient to inactivate the viral infection (Kennedy *et al.*, 2015). Moreover, multiplexed targeting using several sgRNAs targeting the HBV genome at once resulted in more robust suppression of HBV infection (Ramanan *et al.*, 2015).

As already indicated, several groups have used the CRISPR/Cas9 system for elimination of HBV cccDNA from infected cells. They all reported diverse efficiencies since they used different targets within the HBV genome. It is not completely clear how to choose the most efficient target for particular sgRNA. First of all, the accessibility of particular

cccDNA region for the specific sgRNA and the Cas9 protein could vary since the tertiary structure of cccDNA could theoretically be different from cell to cell. Additionally, it was shown that different sgRNAs are more efficient in cleaving the episomal viral DNA while other sgRNAs are rather effective in cleavage of integrated forms of HBV DNA (Ramanan *et al.*, 2015). Furthermore, Lin and colleagues selected several effective sgRNAs against HBV genotype A, but when they applied them on HBV of genotypes B or C they showed completely different results (S. R. Lin *et al.*, 2014). Therefore, it is important to choose conserved and structured cccDNA regions as potential targets for CRISPR/Cas9 (Sun *et al.*, 2010).

It already showed reasonable to target the viral genes that are transcriptionally active (thus accessible) and those whose proteins are easily measurable as HBV antigens at the same time – HBsAg or HBeAg. For example, it was shown that the levels of HBsAg in mouse serum *in vivo* are significantly reduced after treatment with CRISPR/Cas9 system targeting S region of HBV cccDNA (Zhen *et al.*, 2015).

Other successful experiments were performed also *in vivo* in a mouse model using hydrodynamics-based transfection of the CRISPR/Cas9 system. The mice were injected into the tail vein and the CRISPR/Cas9 was transported into the liver by their bloodstream. This subsequently led to a reduction of HBV antigens and cccDNA levels (Dong *et al.*, 2015). There were several other prove-of-concept studies (H. Li *et al.*, 2016; X. Liu *et al.*, 2015; Wang *et al.*, 2015) that overall showed the possibility of CRISPR/Cas9 system to efficiently suppress the viral replication, mutate the viral genome or even destroy the whole cccDNA pool when multiplexed targeting was applied.

In order to transfer the CRISPR/Cas9 system into the clinical use, its efficient delivery has to be solved. Some of the potential delivery systems are described below.

2.3. CRISPR/Cas9 delivery

There are three possible strategies of efficient CRISPR/Cas9 delivery into the cell (Fig. 5). The most widely used method in basic research is CRISPR/Cas9 delivery in the form of plasmid DNA. DNA transfection is typically highly efficient and long lasting, therefore the targeted Cas9 cleavage is very effective (Zhen *et al.*, 2015). However, in potential clinical use, DNA delivery has several important disadvantages. First, plasmid DNA needs to be delivered into the nucleus so there might be a problem with non-dividing cells. Next, there is a high risk of insertional mutagenesis, especially if the viral delivery

systems are used, and most importantly, there is an increased risk of off-target activities due to the long-lasting expression of the Cas9 nuclease. Another option is to deliver the two-component system of the CRISPR/Cas9 consisting of the mRNA encoding Cas9 endonuclease and of the targeting sgRNA (Niu *et al.*, 2014; Yin *et al.*, 2016). In such a case, the expression of Cas9 protein from the mRNA would be limited in time thus decreasing the risk of off-target effects. Secondly, there is no need for nuclear delivery. A big challenge of this strategy represents the diversity of the RNA molecules - the mRNA is about 4.2 kb long whereas the sgRNA has about 100 nucleotides. Accordingly, the last possibility is to co-deliver protein Cas9 together with sgRNA in a form of a ribonucleoprotein complex. The advantage of ribonucleoprotein delivery is their fast mode of action, low cytotoxicity, and immunogenicity and significantly reduced number of off-target events despite the high gene editing efficiency (Zuris *et al.*, 2015).

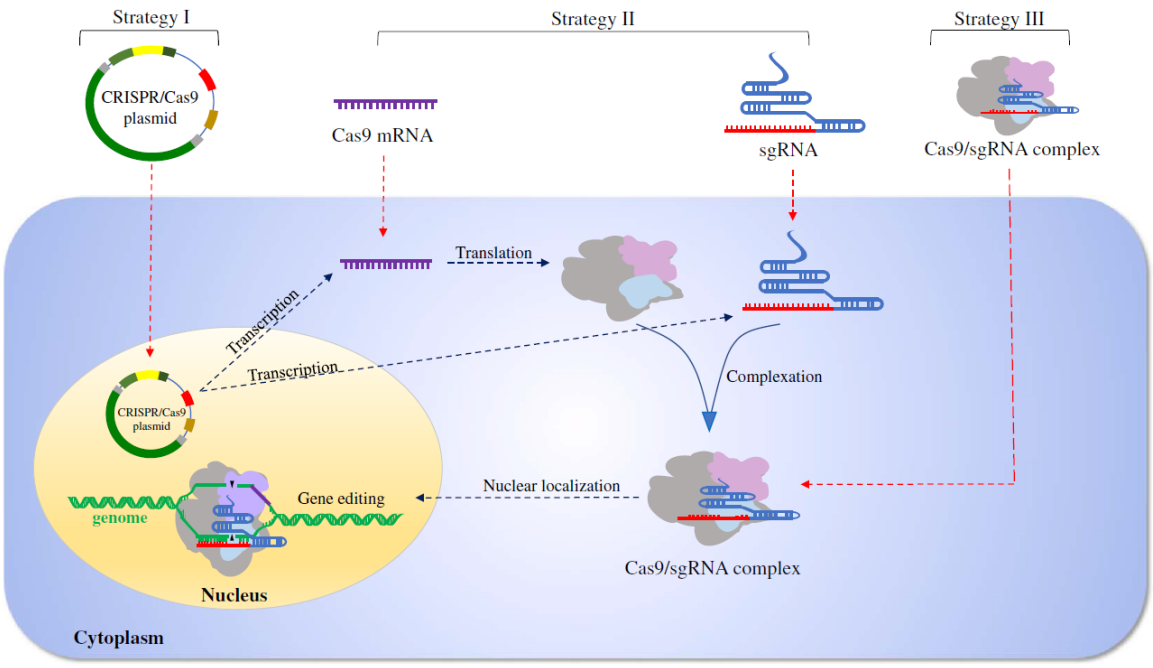

Fig. 5. **CRISPR/Cas9 delivery strategies** – delivery of DNA plasmid, mRNA encoding Cas9 with sgRNA or direct delivery of the final Cas9 protein/sgRNA complex into the cell (adapted from (C. Liu *et al.*, 2017).

From the brief summary above, it is clear that it is desirable to avoid delivery of DNA vectors. On the other hand, RNA delivery seems as the most suitable method for this purpose. It promotes a transient expression of the Cas9 protein, minimizing thus the off-target risks, but it is longer lasting and therefore could be more efficient than protein delivery. Similar to nucleoprotein delivery, there still is a challenge of delivery of different types of molecules (huge mRNA compared to small sgRNA). Still, mRNA encoding Cas9 in complex with

sgRNAs seems to be slightly less problematic compared to Cas9 protein–sgRNA complex delivery. For successful gene editing, it is necessary to transport both sgRNA and mRNA into the same cell, so it is more convenient to mix both components together and pack them inside one nanoparticle. This "all in one" approach is specifically important for potential *in vivo* applications where on could encounter difficulties with lower cellular uptake etc. Nucleic acids generally do not cross the cell membrane in a naked format and despite it was reported that the mRNA can be transported into the cells on its own when administered subcutaneously (Phua *et al.*, 2013), for potential clinical use mRNA needs to be properly delivered. Currently, there are several types of nanoparticles used for mRNA delivery.

2.3.1. Delivery methods

Viral vectors have been studied in detail over the past decades as they can deliver nucleic acids with high efficiencies. Mostly, adeno-associated viruses (AAVs) or lentiviruses are used for DNA delivery. They both are capable of infecting even non-dividing cells with high efficiencies and they are both developed to be non-pathogenic and low-immunogenic. Lentiviral vectors have been used to deliver CRISPR/Cas9 targeting HBV in a number of studies described in chapter 2.2.2. (Ramanan *et al.*, 2015; Seeger & Sohn, 2014). The disadvantage of AAVs for CRISPR/Cas9 delivery is their size-limit packaging, so only truncated Cas9 of *Streptococcus pyogenes* can be used or it needs to be replaced by the smaller Cas9 from *Staphylococcus aureus* (Friedland *et al.*, 2015). The viral systems are great for research purposes, but they do not fulfill demands for *in vivo* applications. The main disadvantage of viral vector still represents the remaining risk of immunogenicity and in case of DNA delivery the risk of insertional mutagenesis.

Highly effective DNA/RNA delivery methods are used *in vitro* such as electroporation, microinjection etc., but they are not suitable for *in vivo* delivery. Hydrodynamic injection is the most convenient technique for nucleic acid delivery in animal models such as mice or rats. The nucleic acid is injected into the tail vein, temporary pores in the membranes of endothelial cells are created and the DNA or RNA can easily enter into the liver (F. Liu *et al.*, 1999). However, this method serves only for experimental purposes. The mRNA delivery is currently of high interest and several mRNA delivery systems have been published such as polymer nanoparticles, gold nanoparticles or lipid nanoparticles. The latter, because of their properties described below, were chosen in our project.

2.3.2. Lipid nanoparticles

Lipid nanoparticles (LNPs) are widely studied transfecting agents as they represent a number of advantages. They are able to efficiently entrap wide spectrum of cargos including both hydrophobic and hydrophilic substances, they are highly stable and biocompatible *in vivo* (Luo *et al.*, 2017). Lipid nanoparticles also reliably protect RNA against degradation by nucleases and they promote their cellular entry by endocytosis or macro-pinocytosis (C. Liu *et al.*, 2017).

Cationic lipids are widely used for the basic composition of lipid nanoparticles due to their ability to bind negatively charged RNA. They also help to promote endosomal escape and intracellular release of the RNA cargo at low pH. These lipids promote RNA condensation and its protection against RNase degradation. Originally, positively charged lipid DOTMA (N-[1-(2,3-dioleyloxy)propyl]-N,N,N-trimethylammonium chloride) (Fig. 6) was developed and used for RNA transfections *in vivo*, but it was later shown to be highly cytotoxic (Malone *et al.*, 1989). The next compound used for liposome assembly with similar properties was DOTAP (1,2-dioleoyloxy-3-trimethylammonium propane chloride) (Fig. 6) (Zohra *et al.*, 2012). Such nanoparticles are suitable for *in vitro* delivery, however, they failed to be effective *in vivo* as they are rapidly absorbed by mononuclear phagocyte system.

Various compounds were later incorporated into LNPs to improve their qualities (Fig. 6). For example, more efficient assembly, reduced aggregation and prolonged blood circulation time of stable nanoparticles can be achieved by adding poly(ethylene)glycol (PEG) layer. Nevertheless, PEG in higher concentrations blocks the cellular uptake and endosomal escape so the exact amount has to be validated. The most promising results are usually obtained when PEG is conjugated with the lipid before the assembly of LNPs. This modification further contributes to the formation of smaller mono-disperse LNPs (Heyes *et al.*, 2006). Furthermore, DOPE (1,2-dioleyol-*sn*-glycero-3-phosphoethanolamine) is often incorporated as a helper lipid to reduce aggregation and improve endosomal escape due to its pH sensitivity. DOPE helps to neutralize the cationic charge of the nanoparticles, promotes membrane destabilization and thus become fusogenic in an acidic environment (Hirsch-Lerner *et al.*, 2005). Additionally, phospholipids can also attribute to the functionality of the lipid nanoparticle by solubilizing small RNAs inside the aqueous pocket of the nanoparticles. Cholesterol is often used as a helper lipid to stabilize the liposome bilayer (Midoux & Pichon, 2015).

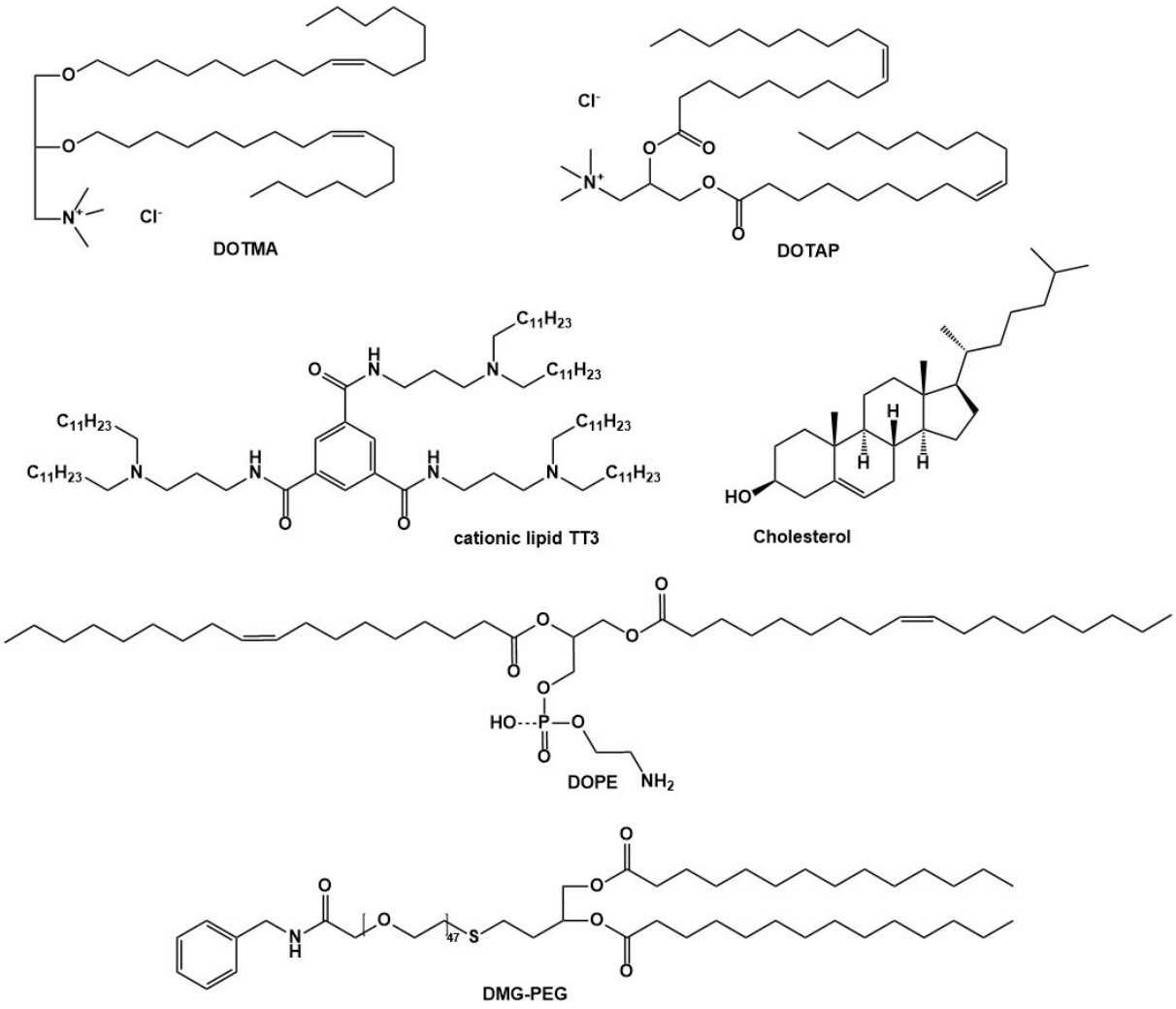

Fig. 6. **Typical components of lipid nanoparticles**. Chemical structures of compounds commonly used for assembly of lipid nanoparticles. The figure shows structures of *in vitro* used DOTMA and DOTAP lipids as well as TT3 lipid, cholesterol, DOPE and DMG-PEG which serve for assembly of recently described nanoparticles for effective mRNA delivery (structures generated by ChemDraw software programme according to literature (B. Li *et al.*, 2015; Mihaila *et al.*, 2011; Yin *et al.*, 2014).

For rapid assembly of high-quality nanoparticles, a new microfluidic device was developed by Li and co-workers (B. Li *et al.*, 2015). The method defines gradual mixing of ethanolic lipid solution with an equivalent volume of aqueous solution containing nucleic acids (Fig. 7). After rapid mixing of both solutions and dilution of ethanol, the solubility of lipids is decreased in water and they self-assemble into LNP while entrapping the nucleic acids through electrostatic interactions. To prevent the aggregation of LNPs, the solution is further diluted with aqueous buffer. LNPs prepared by microfluidic method were shown to be spheroid particles in shape with a narrow distribution of 60-90 nm diameter when mixed with siRNA. That is significantly smaller in diameter than LNPs prepared by normal mixing. This

method is also suitable for nanoparticle preparation in a microliter scale (D. Chen *et al.*, 2012).

By using similar microfluidic device, LNPs of different formulation were tested and evaluated. From those experiments, TT (N^1,N^3,N^5-tris(2-aminoethyl)benzene-1,3,5-tricarbomide) lipids (Fig. 6) were identified as a novel component improving significantly the functions of LNPs. The final composition of LNPs of the best qualities for mRNA delivery is TT3 lipid, DMG-PEG (diacylglycerol-PEG), DOPE and cholesterol (B. Li *et al.*, 2015) (Fig. 6). Nanoparticles composed of these lipids were further tested for example in their ability to co-deliver mRNA and gadolinium (contrast agent for magnetic resonance imaging) *in vivo* (Luo *et al.*, 2017).

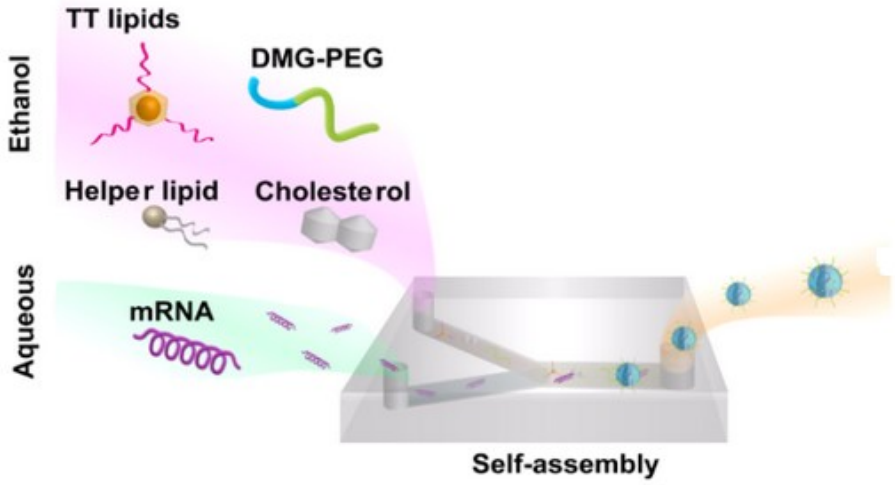

Fig. 7. **Lipid nanoparticle assembly in a microfluidic device** with two inputs – aqueous solution with mRNA and ethanolic solution with a mixture of lipid. After quick mixing, well-defined monodisperse nanoparticles are obtained from the output channel (adapted from (B. Li *et al.*, 2015).

Many other groups are intensively working on CRISPR/Cas9 system delivery. For example, Yin and colleagues showed to co-deliver sgRNA and mRNA using a combination of viral and non-viral components (Yin *et al.*, 2016), but later they improved their system to avoid the viral part for generation of non-immunogenic particles. Furthermore, they improved the properties of sgRNA by several modifications including thioester groups in the phosphate backbone or modifying sugars by using 2'O-methyl ribonucleotide and 2'-deoxy-2'-fluoro-ribonucleotide. According to their results, these modified sgRNAs are more stable against nuclease degradation and enable more efficient gene editing (Yin *et al.*, 2017). Moreover,

during optimization of CRISPR/Cas9 components delivery, new lipid-like compounds were developed by another group. Zwitterionic amino lipids were specially designed to be able to co-deliver long RNAs together with short sgRNAs. The composition of these nanoparticles is similar to other lipid nanoparticles, they contain a cationic lipid, zwitterionic phospholipid, cholesterol, and lipid-PEG. The delivery by this method leads to gene editing with decreased Cas9 protein expression and it was shown that it is efficient both *in vitro* and *in vivo* (J. B. Miller *et al.*, 2017).

In summary, efficient mRNA delivery system has been already developed and optimized for CRISPR/Cas9 delivery. The only remaining step to be solved represents efficient targeting of particular nanoparticles into specific cells in order to minimize the off-target effects of the CRISPR/Cas9 system.

2.3.3. Targeting of liver

Hepatitis B virus is very specific in its tropism, it infects and replicates only in hepatocytes. It is therefore required for an appropriate therapy to focus on these cells and target the therapeutic substances directly to the liver, ideally only to infected hepatocytes. This would bring a huge benefit for CRISPR/Cas9 therapy as most of the CRISPR containing nanoparticles would be transported into the infected hepatocytes and not to any other cell types. In order to do so, it is necessary that the nanoparticle would be able to distinguish hepatocytes from other cell types. Two receptors characteristic for liver cells could possibly serve for targeting. First, the NTCP receptor, which is naturally used by the HBV itself for entry into the hepatocytes, or the asialoglycoprotein receptor (ASGPR).

NTCP, the sodium taurocholate cotransporting polypeptide, (also referred as SLC10A1 as its encoding gene) is a multiple-transmembrane protein of the liver cells and it is a proven interacting partner for viral pre-S1 protein which enables the entry of HBV into the hepatocytes (Yan *et al*. 2012). NCTP has a high affinity for glycine- and taurine-conjugated bile salts and for dihydroxy bile salts (Yan *et al.*, 2014). Numerous molecules interacting with NTCP were identified and some of them were proven to block the HBV entry, however, at the same time they block the bile acid uptake. Cyclosporin A and myrcludex-B were previously mentioned, but there are lots of other compounds, such as for example coumarin derivatives (Kaneko *et al.*, 2018). Similar compounds with the ability to internalize into the cells after binding to NTCP receptor could be theoretically functionalized and attached to the

nanoparticles to enable liver targeting. Such a molecule was already tested in mice for *in vivo* delivery of various cargo compounds such as thyroid hormone analogue (Kersseboom *et al.*, 2017). Some of these interactors were also tested for targeted delivery of various drugs that are metabolized in the liver (Anwer & Stieger, 2014).

ASGPR presents another possibility for liver targeting. ASGPR is a lectin receptor and it can mediate endocytosis of bound inhibitor (on the surface of nanoparticles) via coated pits. The receptor is released from the complex inside endosome and it is transported back to the cell surface. The receptor mediates glycoproteins uptake after Ca^{2+}-dependent galactose/GalNAc (N-acetylgalactosamine) recognition (Lepenies *et al.*, 2013). Several carbohydrate ligands on liposomes were examined, but only multimerized polysaccharides showed positive results as they have a higher number of terminal monosaccharides free for receptor binding (Pathak *et al.*, 2015). Recently, a new inhibitor described as a bicyclic bridged ketal was synthesized and it is reported to target liver with high affinity and ligand efficiency (Sanhueza *et al.*, 2017). The potential of its integration into lipid nanoparticles and CRISPR/Cas9 delivery *in vivo* will be examined.

3. Aims of the Thesis

The aim of this thesis was firstly to design and evaluate CRISPR/Cas9 system enabling editing or degradation of HBV cccDNA and secondly to develop nanoparticles for specific mRNA delivery. If successful, both systems will be later combined together to evaluate their possibilities in HBV treatment.

Specific goals:

- Gene editing of hepatitis B virus by CRISPR/Cas9:
  - Design of new sgRNAs of CRISPR/Cas9 system targeting HBV cccDNA
  - Evaluation of efficiency of plasmid CRISPR/Cas9 cleavage of HBV cccDNA
- Development of mRNA lipid nanoparticles with targeting properties:
  - Assembly of functional lipid nanoparticles
  - Characterization and testing of lipid nanoparticles
  - Specific delivery of nanoparticles by targeting specific cell receptors

4. Materials and Methods

4.1. Materials

4.1.1. DNA

DNA oligonucleotides (synthesized by Sigma-Aldrich):

Primers	
Tag	**Sequence**
S1 guide	CACCGCCCCGCCTGTAACACGAGAA
S2 guide	CACCGTACCGCAGAGTCTAGACTCG
S3 guide	CACCGCAACTTGTCCTGGTTATCGC
S4 guide	CACCGCATTTGTTCAGTGGTTCGTA
C1 guide	CACCGGTGAAAAAGTTGCATGGTGC
C2 guide	CACCGAGCTTGGAGGCTTGAACAGT
C3 guide	CACCGGACCTTCGTCTGCGAGGCGA
C4 guide	CACCGGATTGAGATCTTCTGCGACG
P1 guide	CACCGTGAACCTTTACCCCGTTGCC
P2 guide	CACCGCGGCTAGGAGTTCCGCAGTA
X1 guide	CACCGCGCCGACGGGACGTAAACAA
X2 guide	CACCGGGGGCGCACCTCTCTTTACG
S1 reverse	AAACTTCTCGTGTTACAGGCGGGGC
S2 reverse	AAACCGAGTCTAGACTCTGCGGTAC
S3 reverse	AAACGCGATAACCAGGACAAGTTGC
S4 reverse	AAACTACGAACCACTGAACAAATGC
C1 reverse	AAACGCACCATGCAACTTTTTCACC
C2 reverse	AAACACTGTTCAAGCCTCCAAGCTC
C3 reverse	AAACTCGCCTCGCAGACGAAGGTCC
C4 reverse	AAACCGTCGCAGAAGATCTCAATCC
P1 reverse	AAACGGCAACGGGGTAAAGGTTCAC
P2 reverse	AAACTACTGCGGAACTCCTAGCCGC
X1 reverse	AAACTTGTTTACGTCCCGTCGGCGC
X2 reverse	AAACCGTAAAGAGAGGTGCGCCCCC
pBR322oriF	GGGAAACGCCTGGTATCTTT
Cas9-F	GCATTGGATCCATGGACTATAAGGACCACGACGGAGACTACAA
Cas9-R	GCTATGAATTCTTACTTTTTCTTTTTTGCCTGGCCG
T7 promoter	TAATACGACTCACTATAGGG
T7 terminator (reverse)	GCTAGTTATTGCTCAGCGG
Cas9 sequencing 1	GGTGGTGCTCGAGTGCG
Cas9 sequencing 2	ATCAAGTTCCGGGGCCACTTC
Cas9 sequencing 3	CGGCGGAGCCAGCCAG
Cas9 sequencing 4	GCTGAAAGAGGACTACTTCAAG
Cas9 sequencing 5	GGCCAGAGAGAACCAGACC
Cas9 sequencing 6	GGTGTCCGATTTCCGGAAGG
Cas9 sequencing 7	GGAAGCCAAGGGCTACAAAG

pX333 plasmid was a kind gift from Andrea Ventura (Addgene plasmid # 64073) (Maddalo *et al.*, 2014)

pX330-U6-Chimeric_BB-CBh-hSpCas9 was a kind gift from Feng Zhang laboratory (Addgene plasmid # 42230) (Cong *et al.*, 2013)

pET-24a(+) (Novagen, Cat. No. 69749-3)

pMC.rcccDNA was kindly provided by Dr. Zhi-Ying Chen (Guo *et al.*, 2016)

GelPilot 1 kb ladder (Qiagen, Cat. No. 239085)

GelPilot 100 bp Plus ladder (Qiagen, Cat. No. 239025)

4.1.2. Enzymes

BamHI restriction endonuclease (New England BioLabs, Cat. No. R0136L)

EcoRI HF restriction endonuclease (New England BioLabs, Cat. No. R3101L)

BsaI-HF restriction endonuclease (New England BioLabs, Cat. No. R3535L)

FastDigest BbsI restriction endonuclease (Thermo Fisher Scientific, Cat. No. FD1014)

FastAP – Thermosensitive Alkaline Phosphatase (Thermo Fisher Scientific, Cat. No. EF0654)

Antarctic phosphatase (New England BioLabs, Cat. No. M0289L)

Phusion® High-Fidelity DNA Polymerase (New England BioLabs, Cat. No. MO530L)

- online protocol:https://www.neb.com/protocols/0001/01/01/pcr-protocol-m0530

PPP master mix – Taq polymerase (Top-Bio, Cat. No. P125)

- online protocol: http://www.top-bio.cz/files/1166_pi.pdf

T4 polynucleotide kinase (New England BioLabs, Cat. No. M0201L)

T4 DNA ligase (New England BioLabs, Cat. No. M0202L)

- online protocol: https://www.neb.com/protocols/0001/01/01/dna-ligation-with-t4-dna-ligase-m0202

Quick Ligation™ Kit (New England BioLabs, Cat. No. M2200S)

- online protocol: https://www.neb.com/protocols/0001/01/01/quick-ligation-protocol

RNase A, DNase and protease-free (10 mg/mL) (Thermo Fisher Scientific, Cat. No. EN0531)

4.1.3. Buffers

For the preparation of all buffers and most experiments, autoclaved milliQ water was used from Milli-Q® Integral Water Purification System for Ultrapure Water by Merck (Millipore).

DEPC-treated water – for mRNA work, milliQ water was mixed with 0,1% diethyl pyrocarbonate (Sigma-Aldrich, Cat. No. 40718), incubated at 37 °C overnight and then autoclaved.

TAE buffer, pH 8 - 40 mM Tris (Thermo Fisher Scientific, Cat. No. 15504-020), 20 mM acetic acid (Lach-Ner, Cat. No. 10047-C80), 1 mM EDTA (Sigma-Aldrich, Cat. No. E9884)

TBE buffer, pH 8.3 - 89 mM Tris (Thermo Fisher Scientific, Cat. No. 15504-020), 89 mM boric acid (Penta, Cat. No. 18710-31000), 2 mM EDTA (Sigma-Aldrich, Cat. No. E9884)

PBS, pH 7.4 - 10 mM sodium phosphate dibasic (Lach-Ner, Cat. No. 30061-CP0), 2 mM potassium phosphate monobasic (Lach-Ner, Cat. No. 30016-CP0), 137 mM Sodium Chloride (Penta, Ca. No. 16590-00000), 2,7 mM Potassium chloride (Lach-Ner, Cat. No. 30076-CP0)

6X sample buffer for agarose gels – 10% saccharose (w/v) (Penta, Cat. No. 24970-31000), 0.1% bromphenol blue (Serva, Cat. No. 15375.01)

Citrate buffer – 13 mM, pH 3 (Sodium citrate, Sigma-Aldrich, Cat. No. 1613859)

Lithium chloride – (Sigma-Aldrich, Cat. No. 62476) 8M stock solution was prepared in DEPC-treated miliQ water, then run through a filter (Millex-GP Syringe Filter Unit, 0.22 µm, polyethersulfone, 33 mm, gamma sterilized, Millipore) and aliquots were stored in -20 °C.

LB broth (Thermo Fisher Scientific – Invitrogen ™, Cat. No. 12780-029)

DMEM High glucose – HyClone™ Dulbecco's High Glucose Modified Eagles Medium (GE Healthcare Life Sciences, Cat. No. SH30022.LS)

DMEM complete medium – DMEM High glucose with 10% fetal bovine serum (Gibco™ fetal bovine serum, Thermo Fisher Scientific, Cat. No. 26140-079)

RPMI-1640 Medium (Sigma-Aldrich, Cat. No. 51536C)

Trypsin/EDTA solution for cell dissociation – 0,25% trypsin (Sigma-Aldrich, Cat. No. T4549), 0,2% EDTA (Ethylenediaminetetraacetic acid, Sigma-Aldrich, Cat. No. E6758)

Opti-MEM™ Reduced Serum Medium (Thermo Fisher Scientific, Cat. No. 31985070)

DPBS - HyClone™ Dulbecco's Phosphate Buffered Saline for cell cultures (GE Healthcare Life Sciences, Cat. No. SH30028.LS)

4.1.4. Commercial kits

QIAquick Gel Extraction Kit (Qiagen, Cat. No. 28706)

- online protocol: https://www.qiagen.com/us/resources/resourcedetail?id=3987caa6-ef28-4abd-927e-d5759d986658&lang=en

MinElute PCR purification kit (Qiagen, Cat. No. 28006)

- online protocol: h3ps://www.qiagen.com/us/resources/resourcedetail?id=fa2ed17d-a5e8-4843-80c1-3d0ea6c2287d&lang=en

Gel Extraction QIAEX II kit (Qiagen, Cat. No. 20021)

- online protocol: https://www.qiagen.com/us/resources/resourcedetail?id=13d33145-9f64-426a-a43b-394211d8cf2b&lang=en

ZYPPY™ plasmid miniprep kit (Zymo research, Cat. No. D4020)

- online protocol: https://dwo0hlbtc3ypb.cloudfront.net/amasty/amfile/attach/_D4019_D4020_D4036_D4037_Zyppy_Plasmid_Miniprep_Kit_ver.1.2.7.pdf

HBsAg/HBeAg Hepatitis B Elisa Test Kit (Bioneovan, Cat. No. BE101A, Cat No. BE103A)

- online protocol: https://bioneovan.en.alibaba.com/product/1494327257-211978740/HBsAg_ELISA_Kit.html

AmpliScribe™ T7-Flash™ Transcription Kit (Lucigen (Epicentre), Cat. No. ASF3507.)

- online protocol: http://www.lucigen.com/docs/manuals/MA191E-Ampliscribe-t7-flash-transcription-kit.pdf

4.1.5. Other reagents and chemicals

ARCA – $m_2^{7,3'\text{-}O}GP_3G$ Anti-reverse cap analog (Jena Bioscience, Cat. No. NU-855L)

ssRNA ladder (New England BioLabs, Cat. No. N0362S)

Low range ssRNA ladder (New England BioLabs, Cat. No. N0364S)

GelRed® nucleic acid dye, 10,000X in water (Biotium, Cat. No. 41003)

GenJet™ In Vitro DNA Transfection Reagent (SignaGen®, Cat. No. SL100488)

Lipofectamine™ 2000 Transfection Reagent (Thermo Fisher Scientific, Cat. No. 11668027)

Ampicillin (Sigma-Aldrich, Cat. No. A1000000)

Kanamycin sulfate (Sigma-Aldrich, Cat. No. K1377)

Sepharose 4B (Pharmacia, Fine Chemicals)

Urea (Sigma-Aldrich, Cat. No. U4883)

Acrylamide (Sigma-Aldrich, Cat. No. A3553)

Ammonium persulfate (APS) (Sigma-Aldrich, Cat. No. A3678)

N,N,N′,N′-tetramethylethylenediamine (TEMED) (Sigma-Aldrich, Cat. No. T9281)

Agarose (Serva, Cat. No. 11404.05)

UV ethanol (Lach-Ner, Cat. No. 20025-U99)

COATSOME® ME-81811(DOPE) (NOF America Corporation, Cat. No. 308)

SUNBRIGHT® GM-020 (DMG-PEG) (NOF America Corporation, Cat. No. 329)

1,2-Dimyristoyl-sn-glycerol (Biosynth®, Cat. No. D-5657)

Thiol PEG Acetic Acid (JenKem Technology USA, Cat. No. A5098-5)

Transferrin (Sigma-Aldrich, Cat. No. T3309) with Alexa Fluor™ 488 Sulfodichlorophenol Ester (Thermo Fisher Scientific, Cat. No. A30052) modified by Dr. Jitka Neburková (IOCB, Prague)

TT3 lipid synthesized by Dr. Václav Vaněk (IOCB, Prague) according to the literature (B. Li *et al.*, 2015)

Cholesterol (Sigma Aldrich, Cat. No. 362794)

4.1.1. Bacteria and cell cultures

One Shot™ TOP10 Chemically Competent E. coli (Invitrogen™, Thermo Fisher Scientific, Cat. No. C404010)

Escherichia coli Stbl3 – provided by Dr. Zuzana Kečkéšová (IOCB, Prague)

Huh7 – provided by Dr. Jan Weber (IOCB, Prague) (originally from Okayama University, isolated cells from differentiated hepatoma, age 57, male)

HEK293T – provided by Jana Starková (IOCB, Prague)

U2-OS – provided by Jana Starková (IOCB, Prague)

CEM – provided by Jana Starková (IOCB, Prague)

4.2. Methods

4.2.1. Cloning of CRISPR/Cas9 vectors

Sequences of sgRNAs were first ordered as DNA oligonucleotides (Sigma Aldrich) containing designed overhangs and cloned in dual combinations into the DNA vector pX333 encoding Cas9 protein (Fig. 8) following the recommended cloning protocol for Cas9 vectors from the Zhang laboratory (https://www.addgene.org/crispr/zhang/).

pX333 restriction sites:

BsaI: ...GGACGAAA|CACC GGGTCTTCGAGAAGACCT|**GTTT** TAGAGCTA...
...CCTGCTTT **GTGG**|CCCAGAAGCTCTTCTGGA CAAA|ATCTCGAT...

BbsI: ...GGACGAAA|CACC GGAGACCTATTCGCCTTAAGGTCTCG|**GTTT** TAGAGCTA...
...CCTGCTTT **GTGG**|CCTCTGGATAAGCGGAATTCCAGAGC CAAA|ATCTCGAT...

sgRNA oligonucleotide sequences for cloning:

5′ – **CACCG**NNNNNNNNNNNNNNNNNNN – 3′
3′ – **C**NNNNNNNNNNNNNNNNNNN**CAAA** – 5′

Fig. 8. **Cas9 plasmid pX333 with a sequence containing BbsI and BsaI restriction sites**. Vector encoding gene of Cas9 protein with CMV enhancer and two sites for gRNA insertion under U6 promoters. Insertion sites are followed by gRNA scaffold enabling the formation of CRISPR RNA with a hairpin for activation and binding of Cas9 protein (figure adapted from https://www.addgene.org/64073/). Parts of pX333 sequence containing BsaI and BbsI restriction sites are shown with highlighted recognition sites. DNA is cleaved as indicated by the lines in the gaps, sequences in bold letters are the nascent overhangs. DNA oligonucleotides for cloning were ordered with corresponding overhangs as shown at the bottom.

The pX333 plasmid was digested by FastDigest BbsI (Thermo Fisher Scientific) with FastAP (Thermosensitive Alkaline Phosphatase by Thermo Fisher Scientific) in provided 10×Fast Digest buffer in a total volume of 20 µl for 30 minutes at 37°C. The product was purified on the column from QIAquick Gel Extraction Kit (Qiagen) according to the protocol and analysed on agarose gel (Owl™ EasyCast™ B1 Mini Gel Electrophoresis Systems, Thermo Fisher Scientific; PowerPac™ Basic Power Supply, Bio-Rad) (0,6% agarose, GelRed dye, TAE buffer, 40min/120V, Gel Pilot 1 kb ladder).

The concentration of plasmid was analyzed using NanoDrop2000 spectrophotometer (Thermo Fisher Scientific). DNA oligonucleotides (both 10 µM) were annealed while mixed with T4 polynucleotide kinase (NEB) in 10×T4 ligation buffer in total volume of 10 µl in a thermocycler (Biometra Trio, Analytik Jena) (37°C for 30 min, then 95°C for 5 min and then cooled down to 25°C at 1°C/12 s). Ligation reaction contained digested plasmid, phosphorylated and annealed oligo duplex, QuickLigation buffer and Quick Ligase (Quick Ligation™ Kit, NEB) and it was incubated for 10 minutes at room temperature.

Bacterial transformation

Bacterial strain Stbl3 was transformed with the cloning product by heat shock reaction. Ligated DNA was added to bacteria suspension and incubated for 10 minutes on ice, then for 1,5 min at 42°C and then transferred on ice for 2 min. The mixture was diluted with 250 µl of LB media, incubated at 37°C for 1 hour (Peltier-cooled incubator IPP400, Memmert) and then spread on agarose plate with ampicillin (100 µg/ml). As a positive control, bacteria with original pX333 were used whereas bacteria with digested pX333 served as a negative control. The bacteria on plates were incubated at 37 °C overnight.

Colony PCR

To analyze the cloning reactions, two colonies of each sample were selected from the agarose plate, touched with a sterile tip on a pipette and resuspended in 10 µl of milliQ water. 1 µl of the suspension was used for colony PCR performed using PPP master mix (including Taq polymerase, Top-Bio s.r.o.) with pBR322oriF sequencing primer and reverse complementary sgRNA oligonucleotides following these conditions:

	Temperature	Time [min:s]
	94°C	10:00
35 cycles	94°C	0:15
	52°C	0:30
	72°C	0:30
	72°C	7:00

The result of colony PCR was analyzed on an agarose gel (1,2% agarose, GelRed dye, TAE buffer, 110V/30min) with a DNA molecular length marker Gel Pilot 100 bp Plus ladder. Expected length of PCR products is 480 base pairs.

Minipreparation

Plasmids with inserted sgRNA oligos were amplified by minipreparation. Bacterial colonies were previously resuspended in 10 µl of milliQ water. Five µl of this suspension were pipetted into 8 ml of LB media with of ampicillin (100 µg/ml). The reaction was incubated in a shaker (New Brunswick™ Innova® 44/44R, Eppendorf) at 37°C overnight, then centrifuged (3500×g, 10 min, 15°C). The supernatant was discarded and the bacterial pellet was resuspended in 600 µl of milliQ water. The DNA was extracted using ZYPPY™ plasmid miniprep kit (Zymoresearch). The concentration of plasmid with the first sgRNA was analyzed using NanoDrop2000 (Thermo Fisher Scientific) and sent for sequencing to GATC, Biotech with pBR322oriF sequencing primer. The whole procedure was repeated with BsaI-HF restriction endonuclease (NEB) to insert second sgRNA DNA oligo. Dephosphorylation of plasmids was performed as a second step after digestion using Antarctic phosphatase (NEB, incubation for 30 min at 37°C). The final products were also sequenced by GATC Biotech.

4.2.2. HBV infection

In order to test our CRISPR/Cas9 system by a more robust method than the typical (usually inefficient) viral infection, we used recombinant cccDNA (rcccDNA) encoding infectious HBV. This rcccDNA can be reproduced in high quantities in bacteria like other plasmids and it can be further transfected into mammalian cells using common transfecting reagents. Once in a mammalian cell, it forms a cccDNA structure inside the nucleus and it produces all HBV transcripts leading to assembly and release of functional infectious viruses (Guo *et al.*, 2016). Recombinant cccDNA was amplified from the pMC.rcccDNA vector depicted in Fig. 9 by Dr. Barbora Lubyová in the BSL3 lab at IOCB Prague. All procedures

starting with the cell transfection with rcccDNA, followed by CRISPR treatment and efficacy evaluation, were performed at IOCB virology laboratory of biological safety level 3.

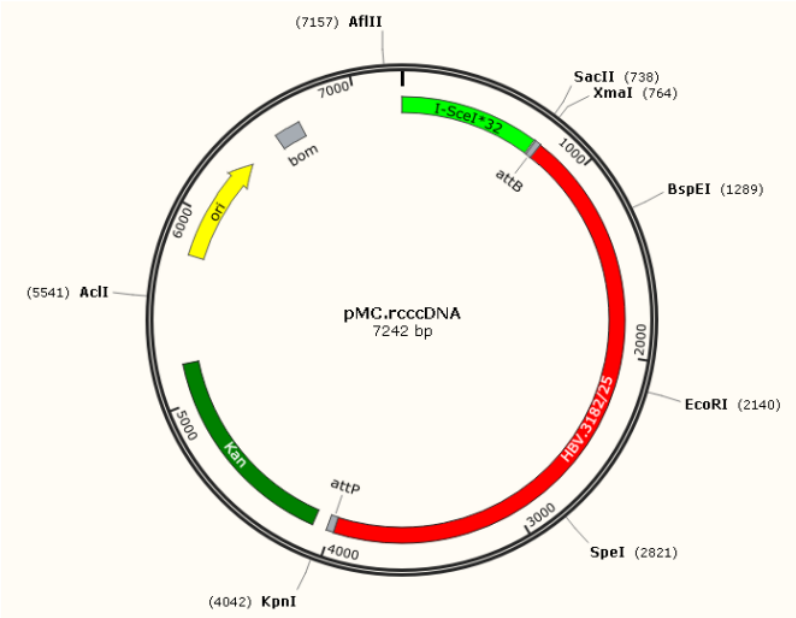

Fig. 9. **Plasmid encoding recombinant rcccDNA of HBV.** The plasmid can be produced in bacteria and it encodes kanamycin resistance for positive selection. Once it is in a eukaryotic cell, it forms the cccDNA structure and remains in the cell nucleus even after cell division (adapted from (Guo *et al.*, 2016).

4.2.1. Huh7 transfection

All experiments containing work with cell lines were carried out in a laminar flow box (Clean Air®, Telstar) for cell cultures. Huh7 cell culture was maintained in an incubator (5% CO_2, Sanyo) at 37°C in DMEM complete medium prepared by Jana Starková (IOCB Prague). For transfection of DNA, GenJet reagent (SignaGen®) was used. Experiments were performed *in vitro* in a 12-well plate format. Each well was seeded with 180 000 cells in 1 ml of DMEM complete. Each well with the cells was transfected with DNA mixture (HBV rcccDNA and CRISPR/Cas9 vector, 3:10 ratio) in 3 µl of GenJet reagent (1:3 ratio). DNA and GenJet were mixed in DMEM High glucose in a total volume of 100 µl per sample and incubated for 15 minutes at room temperature before transfection. For a control, cells were transfected with pX333 plasmid without targeting sequence inserted, rest of the cells were transfected by 10 different combinations of sgRNA cloned into the pX333 vector. Each sample was presented in a triplicate. The media with transfection mixtures were removed 1 day after transfection, the cells were washed twice with 2 ml of PBS and 1 ml of fresh DMEM complete was added. The cells were incubated at 37°C until day 6 post transfection when the media containing viral antigens were collected and centrifuged (5000×g, 5 min,

15°C). Collected supernatants were stored in the -80°C freezer. One ml of fresh DMEM complete was added and the cells were incubated six more days until day 12 post infection when the media were harvested again. The levels of viral antigens were measured on ELISA.

4.2.2. ELISA detection of HBV antigens

Viral antigens (HBsAg and HBeAg) were measured from the media harvested from the cells 6 and 12 days post infection using HBsAg/HBeAg Hepatitis B Elisa Test Kits (Bioneovan) in 96-well plates according to the manufacturer protocol. The wash steps were performed using automatic microplate washer (HydroFlex™, Tecan). HRP-conjugate is used for detection of viral antigens, so the results were analyzed on a fluorescent plate reader (Victor X3, PerkinElmer) at 450 nm. Only relative levels of antigens in sera are obtained by this method. The sample transfected only with rcccDNA of HBV was considered as 100 % infection and samples transfected with CRISPR/Cas9 were compared with this number.

4.2.3. Preparation of mKate2 and Cas9 DNA for transcription

For functionality tests of lipid nanoparticles, mRNA encoding fluorescent protein mKate2 was used for easy detection instead of the mRNA encoding Cas9. For *in vitro* transcription, T7 RNA polymerase was used, so DNA of mKate2 was cloned into the pET24a with T7 promoter by Jan Belza (IOCB, Prague). Similarly, Cas9 was further cloned into the pET24a as well:

Cas9 gene was obtained from the pX330 Addgene vector by PCR reaction with Phusion polymerase (NEB) in provided 5×HF buffer in a total volume of 30 µl. Gene was multiplied using primers for Cas9 cloning (Cas9-F, Cas9-R) described in the material list. Primers contained sequences for further cleavage by restriction endonucleases EcoRI or BamHI.

The PCR was set along these conditions:

	Temperature	Time [min:s]
	98°C	0:30
35 cycles	98°C	0:10
	59°C	0:20
	72°C	3:00
	72°C	7:00

PCR product was loaded on an agarose gel (0,5% agarose, GelRed dye, TAE buffer, 40min/150V, Gel Pilot 1 kb marker). The DNA band corresponding to Cas9 gene (approximately 4,2 kbp) was cut off the gel and DNA was purified using Gel Extraction QIAEX II kit (Qiagen) according to provided protocol.

Cas9 DNA and pET24a were both digested by EcoRI HF (NEB) in provided 10×NEB 2.1 buffer in a total volume of 20 µl for 2 hours at 37°C. Later, DNA was purified using MinElute PCR purification kit (Qiagen). In the next step, both DNA molecules were digested by BamHI restriction endonuclease (NEB) in 10×NEB 2.1 buffer in a total volume of 25 µl for 2 hours at 37°C. Cas9 DNA was purified again via MinElute PCR purification kit. Antarctic phosphatase was added with its 10×buffer into the digested pET24a and the reaction was incubated for 30 min at 37°C. The digested plasmid was loaded on an agarose gel (0,5% agarose, GelRed dye, TAE buffer, 40min/150V, Gel Pilot 1 kb marker) and purified using Gel Extraction QIAEX II kit. Both insert and plasmid were mixed together with T4 DNA ligase (NEB) in its 10×buffer in a total volume of 20 µl and ligated at 16°C overnight.

Bacterial transformation and minipreparation

E. coli TOP10 cells were used to amplify the plasmid with Cas9 gene. Bacteria were transformed by heat shock reaction described in chapter 4.2.1. and then they were spread onto an agarose plate with kanamycin (40 µg/ml). As described in chapter 4.2.1., colony PCR and minipreparation were performed in the same way. Bacteria for minipreparation were incubated in 8 ml of LB medium with kanamycin (40 µg/ml). The cloning result was verified by GATC, Biotech sequencing.

Preparation of Cas9 DNA for *in vitro* transcription

Cas9 gene was amplified with the T7 promoter and terminator primers from pET24a by PCR reaction with Phusion polymerase (NEB) in provided 5×HF buffer in a total volume of 20 µl.

The PCR was set along these conditions:

	Temperature	Time [min:s]
	98°C	0:30
35 cycles	98°C	0:10
	59°C	0:20
	72°C	3:00
	72°C	7:00

4.2.4. *In vitro* transcription

All experiments containing RNA including the preparation steps were performed in the sterile environment in laminar flow box (Clean Air®, Telstar) selected for RNA work. The RNA of mKate2 and Cas9 were prepared using AmpliScribe™ T7-Flash™ Transcription Kit (Epicentre) according to the manufacturer protocol with the addition of ARCA (Anti Reverse Cap Analog, Jena Bioscience) (Jemielity *et al.*, 2003). As a template served DNA with T7 promoter prepared by previous cloning and PCR multiplication described above. After the transcription reaction, RNA was treated with DNaseI as additional step described in the protocol of the kit. RNA was purified by precipitation with lithium chloride. LiCl was added to the reaction (final concentration 3.6M), the reaction was incubated at -20 °C for 30 minutes and then centrifuged (20000×g, 5 min, 4°C). The pellet was washed with 500 µl of 70% ethanol and let dry in open Eppendorf tube for 10 minutes, then it was resuspended in DEPC-treated milliQ water. Subsequently, RNA was treated with RNA poly(A)polymerase for the addition of 150-200 adenines to 3'end to mimic endogenous mRNA and to prevent activating of restriction reactions inside the cells. To improve the yields, 1 µl of RNA poly(A) polymerase (produced in yeast, Affymetrix) was used for polyadenylation of 30 µg of purified RNA and incubated at 37 °C for 2 hours (in provided buffer, ATP final concentration 1 µM, RNase inhibitor from transcription kit added). Final mRNA containing cap and poly(A)tail was purified using LiCl as described above and analyzed by gel electrophoresis.

4.2.5. RNA Polyacrylamide gel electrophoresis

In order to analyze RNA with and without poly(A) tail, polyacrylamide electrophoresis was performed (Mini-PROTEAN® Tetra Cell, Bio-Rad). Stock solution for RNA PAGE (urea 10% w/v and acrylamide 4,75% w/v in TBE) was mixed and quickly heated in the microwave to dilute all crystals and then immediately put on ice to cool down. The solution calculated for one gel was prepared by adding ammonium persulfate (APS, 0,1% w/v) and N,N,N′,N′-tetramethylethylenediamine (TEMED, 0,2% v/v) and applied between two glasses for electrophoresis with a comb. After about 1 hour, the comb was removed and the wells were rinsed with TBE buffer. 100 ng of each RNA sample was analyzed. The samples were first mixed with RNA loading dye (NEB) in a total volume of 10 µl, incubated at 95°C for 5 minutes, quickly cooled on ice, spun down in a centrifuge and then loaded on the gel. As a control, ssRNA ladder and LowRange ssRNA ladder (NEB) were used. The electrophoresis

was performed at 900 V for about 15 minutes while there was a cooling pack inside the tank and the apparatus was placed on a magnetic stirrer – one stirrer was placed between two glasses with gels and the second one on the bottom of the electrophoresis tank. The gel was stained after the electrophoresis in a solution of GelRed (Biotium) and visualized on UV transilluminator (Quantum-ST4-1100, Vilber Lourmat).

4.2.6. Lipid nanoparticles assembly

Lipids for nanoparticles were provided by Dr. Cigler group (IOCB Prague, Laboratory of synthetic nanochemistry). The final composition of lipid mixture was cholesterol, DOPE, TT3 lipid and DMG-PEG (4:3:2:1 ratio) according to the literature as described in chapter 3.3.2. Lipids were supplied in 99% ethanol. LNPs were assembled using the microfluidic device with two inputs (1:1 volume ratio) – first was the lipid mixture in ethanol, second was a solution containing mRNA encoding mKate2 in 10 mM citrate buffer, pH 3. At first, these two solutions were forced into the microfluidic device from the syringes using mechanical push, later on, they were applied into Hamilton syringes and forced by the automatic pump at a flow rate of 300 μl/min. Output wire was connected with microtube on magnetic stirrer containing PBS (1:1 ratio with total volumes of both inputs).

4.2.7. Dynamic light scattering analysis of LNPs

The critical method for evaluating the quality of new LNPs was DLS measurement using Zetasizer Nano ZS instrument (Malvern Panalytical). For diameter analyses and relative count rate of nanoparticles, samples were 10X diluted in PBS and applied in disposable polystyrene cuvette. For determination of zeta potential, samples were 10X diluted in milliQ water and measured with Universal 'Dip' Cell Kit (Malvern, Panalytical).

4.2.8. Addition of targeting moiety via click chemistry

For prove-of-principle studies of LNPs targeting specific cell receptors, transferrin was chosen as a model system. Transferrin was added to the surface of LNPs later after assembly by click reaction (Taylor *et al.*, 2011). For these reasons, DMG-PEG with free tetrazine and

transferrin with trans-cyclooctene were synthesized by Dr. Cigler's group. These new LNPs assembled in a microfluidic device containing DMG-PEG-tetrazine were further mixed with modified transferrin and incubated at 4 °C overnight on the rotator. LNPs were then purified from unbound transferrin on Sepharose 4B column.

4.2.9. Purification of LNPs on sepharose column

Sepharose 4B was obtained pre-swelled in 20% ethanol (Pharmacia, Fine Chemicals). 15 g of Sepharose was resuspended in 5 ml of PBS and degassed in a vacuum flask. Afterward, it was carefully but quickly poured into the column over glass rod. The column was washed with at least 20 ml of PBS which was constantly flowing in from another column placed above the sepharose column on a lab stand. When the beads settled down, the PBS inflow was stopped and the level of PBS above the sepharose beads was dropped out until it reached the beads level. The LNPs sample after the click was then applied onto the sepharose column carefully to not swirl the beads. The sample was let to soak into the beads and then the column was topped with PBS until full. Fractions of 0,5 ml were collected from the column with an instant inflow of PBS.

All fractions from sepharose column were further analyzed, fractions containing LNPs with clicked transferrin were identified in a spectrophotometer at 280 nm (Specord® 250 Plus, Analytik Jena) or according to fluorescence of clicked transferrin-Alexa488 on fluorescence microplate reader (Infinite M1000, Tecan) with Magellan software. These positive fractions were also analyzed on DLS instrument for relative count rate.

4.2.10. Cell transfections with LNP

LNPs were successfully transfected into U2-OS and Huh7 cell lines. Transfection was usually analyzed in 96-well plate format. Cells were seeded in the plate one day before transfection. A mixture of LNPs was slowly dropped from a pipette tip over the well. For a positive control, 100 ng of mRNA was transfected using commercial reagent Lipofectamine2000 (Thermo Fisher Scientific) (0,3 µl per well – 1:3 ratio, mixed with mRNA in Opti-MEM and incubated for 25 minutes at room temperature before transfection), for a negative control cells without transfection were prepared to set a background for cytometer measurement. The cells were incubated with the transfection mixture for 20 hours at 37°C.

Then the medium was removed, cells were washed with DPBS and trypsin/EDTA solution was added. After cell dissociation, DMEM complete was added and the whole mixture was transferred into the 96-well plate with U-bottom for cytometer measurement which was performed as soon as possible after that.

Moreover, CEM cells were used for LNP transfection. CEM were maintained in RPMI medium. CEM is a suspension cell line, so the plate with cells was centrifuged (350×g, 5 min) and the cells were then washed by PBS to remove the transfection mixture, centrifuged again and diluted with the medium before cytometry measurement.

4.2.11. Cytometer analysis of LNPs transfection

Samples were measured using BD LSRFortessa™ flow cytometer (BD Bioscience) on high throughput screening mode in 96-well plates. Appropriate voltage, flow rates, and other conditions were set with help of Jana Gunterová (IOCB Prague) who is trained in cytometer maintenance. For evaluation of delivery efficiency, the fluorescence of mKate2 was measured (561-610/20). Positive signal of mKate2 means that the nanoparticles entered the cells, released the mRNA cargo and the mRNA was successfully translated into the protein. Furthermore, in case of nanoparticles which contained targeting molecule of transferrin fused with Alexa488, the ratio of the cell which took in the nanoparticles could be observed (488-530/30). Results were analyzed using BD FACSDiva™ software programme.

4.2.12. RNAse treatment of LNPs with mRNA

The mRNA encoding mKate2 was treated for 5 minutes with RNase A of different concentrations and analyzed on RNA PAGE to identify effective digestion conditions. LNPs assembled from the microfluidic device were then treated with RNase A of selected concentration for up to 3 hours at 37°C and then transfected into the cells and after 20 hours measured on cytometer, as usual, to prove that LNPs can efficiently protect RNA against RNase degradation.

5. Results

5.1.1. CRISPR/Cas9 design and cloning

For effective HBV genome targeting, conserved regions of serotype ayw were selected according to the literature (Sun *et al.*, 2010) with emphasis on overlapping sequences encoding two HBV proteins simultaneously. The sgRNA sequences within the chosen regions were then generated using CRISPR online design tool (http://crispr.mit.edu/). Twelve different sgRNAs (Table 1) (Fig. 10) were selected – four sgRNAs targeting the S region overlapping with P gene, four sgRNAs targeting the C region overlapping with P gene, two sgRNAs targeting X gene together with P gene and finally two sgRNAs targeting P gene only. All of these sgRNAs were predicted with the lowest ratio of possible off-targets within human genome while they were targeting regions the most conserved within different HBV "species". The sequences were also checked in online HBV database (https://hbvdb.ibcp.fr/HBVdb/HBVdbIndex) to verify if they target most of the genotypes.

Table 1: **Sequences of selected sgRNAs targeting HBV.** Sequences were named according to the viral proteins which they target. Sequences are shown with following PAM sequence (marked in green) which is presented in HBV genome and it is not a part of sgRNA oligonucleotides.

Tag	gRNA sequence
P1	CGCCGACGGGACGTAAACAAAGG
P2	CGGCTAGGAGTTCCGCAGTATGG
X1	GGGGCGCACCTCTCTTTACGCGG
X2	TGAACCTTTACCCCGTTGCCCGG
C1	GATTGAGATCTTCTGCGACGCGG
C2	GACCTTCGTCTGCGAGGCGAGGG
C3	GTGAAAAAGTTGCATGGTGCTGG
C4	AGCTTGGAGGCTTGAACAGTAGG
S1	CCCCGCCTGTAACACGAGAAGGG
S2	TACCGCAGAGTCTAGACTCGTGG
S3	CAACTTGTCCTGGTTATCGCTGG
S4	CATTTGTTCAGTGGTTCGTAGGG

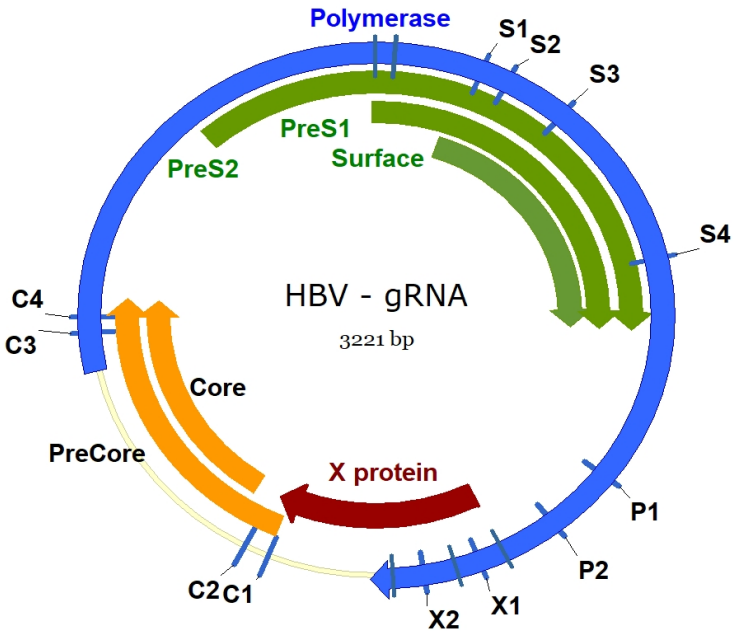

Fig. 10. **Selected sgRNA sequences targeting HBV genome**. HBV genome of ayw serotype is shown with encoded viral proteins to visualize overlapping targets of sgRNAs (figure created in Vector NTI software).

Twelve chosen CRISPR RNA guides were obtained as DNA oligonucleotides and cloned into the vector pX333 in ten different dual combinations (Table 2). The plasmid pX333 was first digest by BbsI restriction endonuclease and purified on agarose gel (Fig. 11) and half of the sgRNAs (first part of dual combinations) were inserted and analysed on agarose gel (Fig. 12). After sequencing and minipreparation, the plasmids with inserted sgRNAs was cleaved by BsaI endonuclease and the second sgRNA oligonucleotides were inserted and analysed on gel in similar manner. The cloning products were verified by sequencing.

Table 2: **Dual combinations of sgRNA sequences in pX333 vector** inserted within the gRNA scaffolds.

sgRNA combinations	
S1–P2	C2–X1
S1–C3	C2–S4
S2–C4	X2–C1
S3–P1	X2–C3
S3–C4	X2–S4

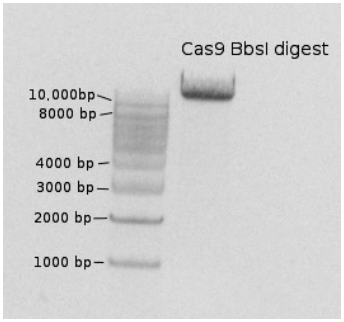

Fig. 11. **Cas9 plasmid pX333 after cleavage by BbsI restriction endonuclease.** Cas9 vector with 8990 bases in total containing dual scaffold for sgRNA was first cleaved by BbsI restriction endonuclease to insert the first oligonucleotide and analyzed on agarose gel electrophoresis.

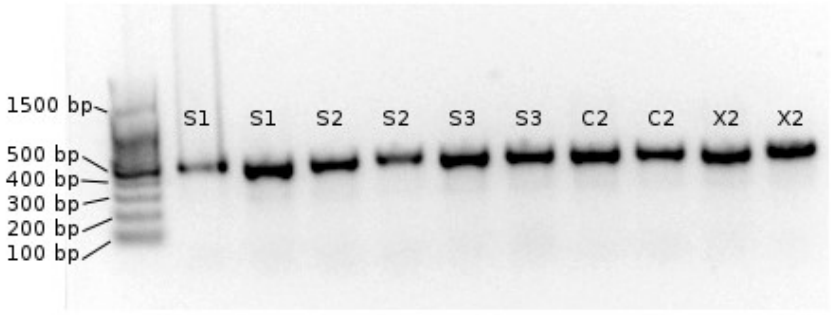

Fig. 12. **pX333 plasmid with inserted CRISPR guide RNA sequences.** Agarose gel electrophoresis showing colony PCR of pX333 digested with BbsI and with inserted CRISPR guides (tagged S1, S2, S3, C2, and X3 according to hepatitis B viral proteins which they target).

5.1.2. Evaluation of CRISPR/Cas9 cleavage of HBV cccDNA

Recombinant cccDNA encoding HBV was used for effective testing of CRISPR/Cas9 efficacy. Huh7 cells were transfected with rcccDNA and viral antigens HBeAg and HBsAg were measured after six days to verify production of viral proteins. Later, rcccDNA was co-transfected to Huh7 cells together with the pX333 plasmid with dual guides. One day after, medium with transfection mixture was discarded and cells were washed to stop the transfection and to prevent cytotoxicity effects of GenJet. Cleavage of rcccDNA was evaluated by a decrease of HBeAg and HBsAg levels (Fig. 13) measured by ELISA. Each sample was presented in triplicate and the whole experiment was repeated three times. In the first experiment (ZK1), cells were discarded after six days post transfection. After ELISA measurement, it was shown that levels of HBsAg are not sufficient for the measurement, therefore in the next experiments (ZK2, ZK3), cells were incubated for twelve days in total.

Only results from two experiments after twelve days are shown for HBsAg. HBeAg levels were measured after 6 days in the first experiment and after 6 and 12 days in the next two experiments.

A

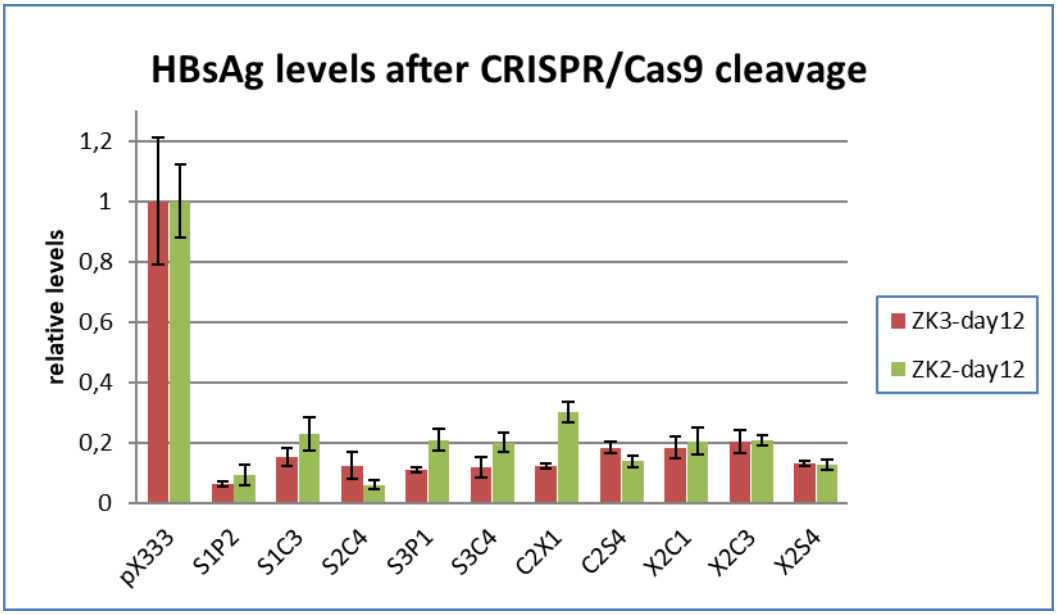

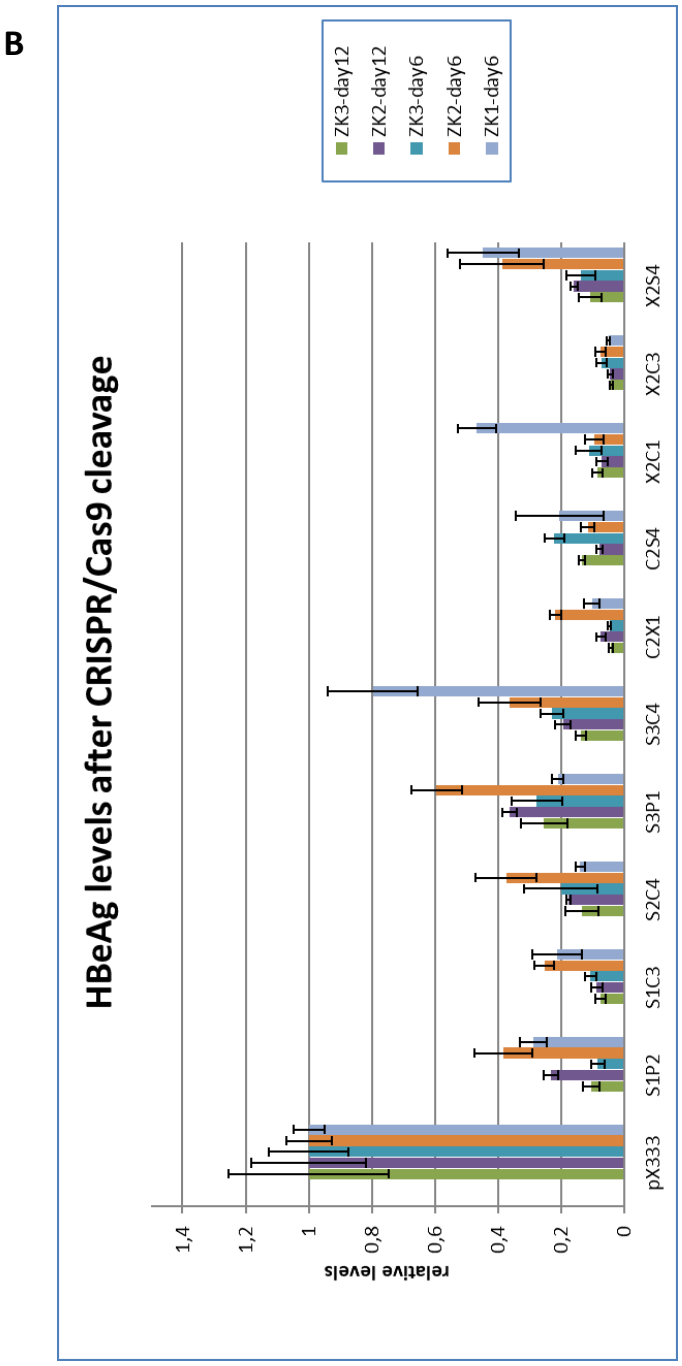

Fig. 13. **Evaluation by ELISA of CRISPR/Cas9 cleavage of HBV rcccDNA**. For control, Huh7 cells were transfected with HBV rcccDNA and empty pX333 vector without targeting sequence. Antigens were collected on day 6 and day 12 post infection. Control sample was considered as 100% infection, the reduction of antigen levels was related to this value. Bars indicate average values from triplicates with standard deviations. **A** HBsAg is produced later in the viral cycle, so the levels on the day 6 post infection is below the detection rate of available ELISA diagnostic kit. The results from 2 experiments are shown. **B** Levels of HBeAg from day 6 after transfection from three experiments and from day 12 after transfection from two experiments are shown.

5.1.3. Preparation of mRNA for lipid nanoparticles

Genes encoding mKate2 and Cas9 were cloned under the T7 promoter to enable further transcription by T7 RNA polymerase. The mKate2 with T7 promoter was previously prepared by a colleague from the laboratory, Jan Belza. Gene for Cas9 was amplified from the pX330 plasmid and purified on an agarose gel (Fig. 14). The purified gene was cloned into the pET24a plasmid under the T7 promoter.

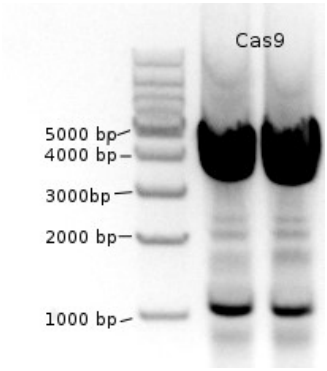

Fig. 14. **Cas9 PCR product for cloning into pET24a.** Cas9 was amplified from the pX330 plasmid using primers (Cas9-F, Cas9-R) which contained restriction sites for BamHI and EcoRI for further cloning into pET24a between the T7 promoter and T7 terminator.

As a cargo for lipid nanoparticles, mRNA of mKate2 and Cas9 was prepared by *in vitro* transcription with addition of cap analogue and poly(A)tail by poly(A)polymerase. High quantities of mKate2 mRNA were successfully transcribed and tested via polyacrylamide gel electrophoresis (Fig. 15). Gene encoding mKate2 consist of 788 nucleotides, mRNA should be approximately 150-200 longer because of poly(A) tail. Cas9 gene is more than 4 kbp long and it was not possible to visualize the mRNA by available methods.

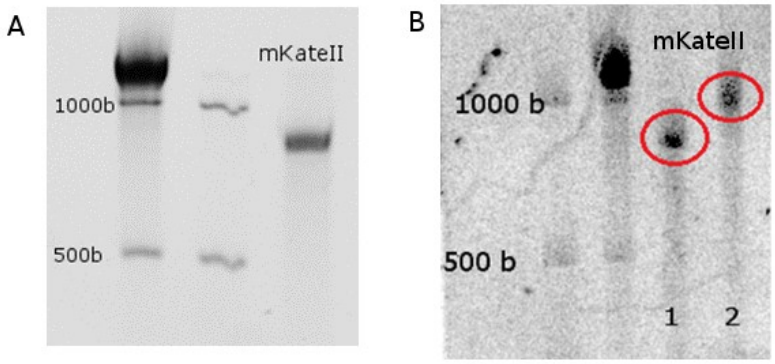

Fig. 15. **Polyacrylamide gel electrophoresis visualization of mRNA encoding mKate2.** ssRNA ladder and Low Range ssRNA ladder were used as RNA length markers. **A** mKate2 mRNA should be approximately 950 bases long depending on the poly(A) tail length. **B** Two mKate2 RNA forms are shown in red circles – before (1) and after (2) polyadenylation.

5.1.4. Preparation and characterization of lipid nanoparticles

After mRNA preparation and its evaluation on gel electrophoresis, lipid nanoparticles were produced. 120 µg of mKate2 was used for the first experiments performed with IOCB in-house prepared microfluidic device. Assembled nanoparticles were characterized by DLS. Typically, all samples were 10X diluted for the DLS measurement. The average diameter of nanoparticles containing mRNA from several experiments was around 200 nm (Fig. 16). To obtain a real visual image of the nanoparticles, a sample for transmission electron microscopy (TEM) was prepared (Fig. 17) and analysed by Jan Vávra (IOCB Prague). Samples were stained with 2% phosphotungstic acid and dried. Although the lipid nanoparticles slightly change their appearance after dehydration, the image from TEM corresponds nicely to the results obtained by DLS. Most of the nanoparticles visible in TEM image, are of 200 nm in diameter. Additionally, a number of smaller nanoparticles could be detected. The peak from DLS is not fully monodisperse, so there might be many small assembled lipid nanoparticles or micelles without significant signal for the DLS measurement or it may be an artifact caused by sample dehydration.

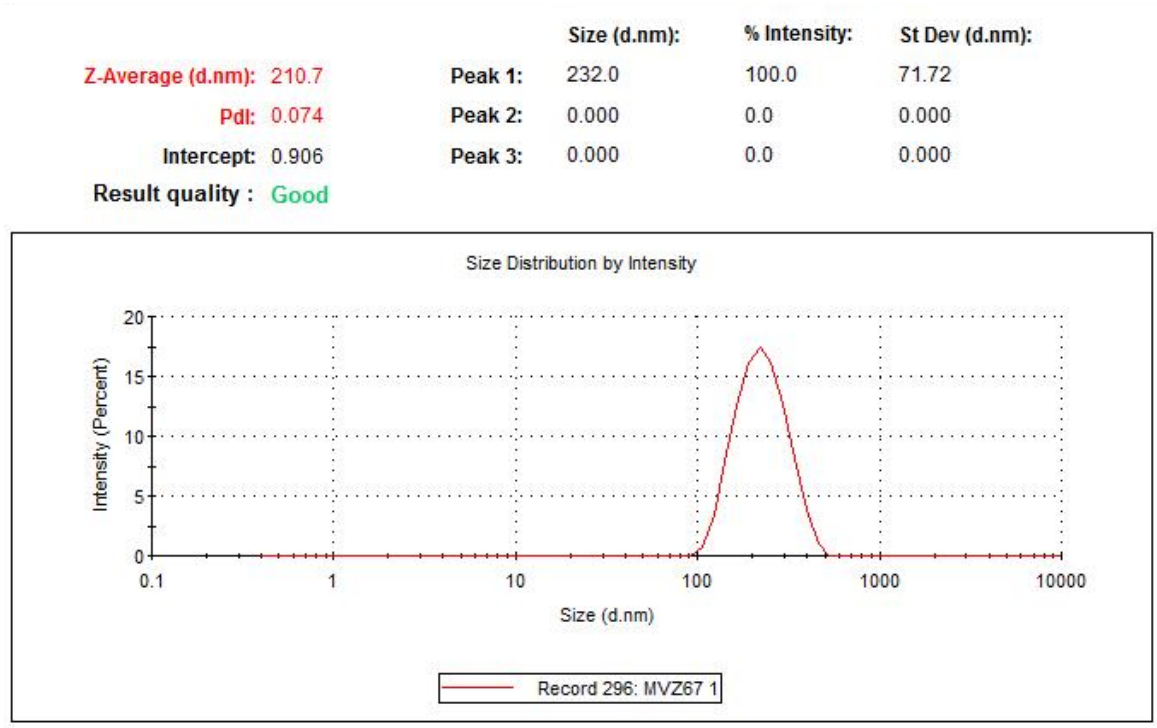

Fig. 16. **DLS measurement of LNPs.** The output from DLS software is shown with a curve showing LNPs with the relatively narrow distribution of average diameters.

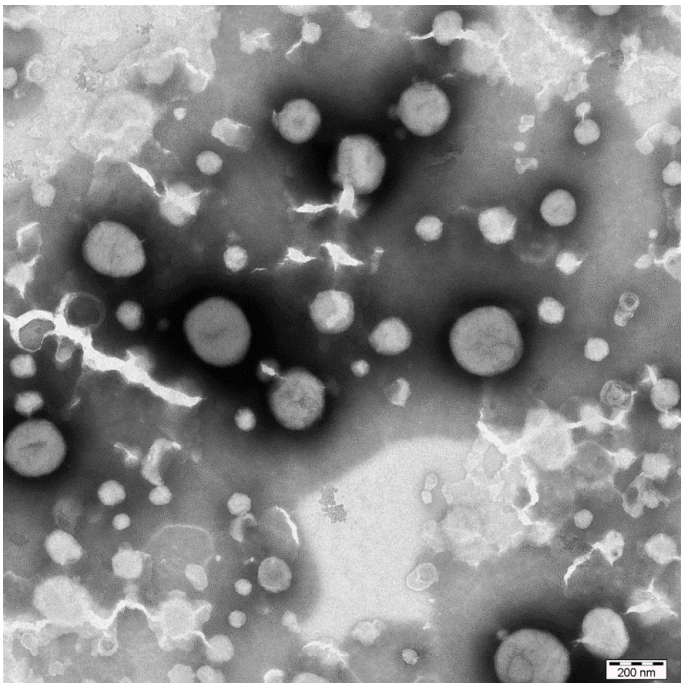

Fig. 17. **TEM visualization of LNPs.** The scale of 200 μm shown in the right lower corner. The picture was taken by Jan Vávra.

The channels for solution mixing were too wide in our microfluidic device so it was necessary to make them thinner in order to obtain smaller particles. Since IOCB does not have an appropriate technology to do so, new microfluidic device was obtained from uFluidix company according to our instructions (Fig. 18). The new device was connected with an automatic pump for Hamilton syringes (with input solutions) which enabled to establish a stable flow rate during LNPs assembly. Nanoparticles obtained by a new device were smaller with more narrow distribution of average diameters (Table 3).

Table 3: **Average diameter and zeta potential of LNPs** measured on DLS instrument. Comparison of results obtained from two different microfluidic devices - from IOCB workshop and from the uFluidix company.

	diameter (nm)	Zeta potential (mV)
IOCB device	193,2	-16,1
	210	-14,6
uFluidic device	145,8	-0,781
	165,1	-4,71

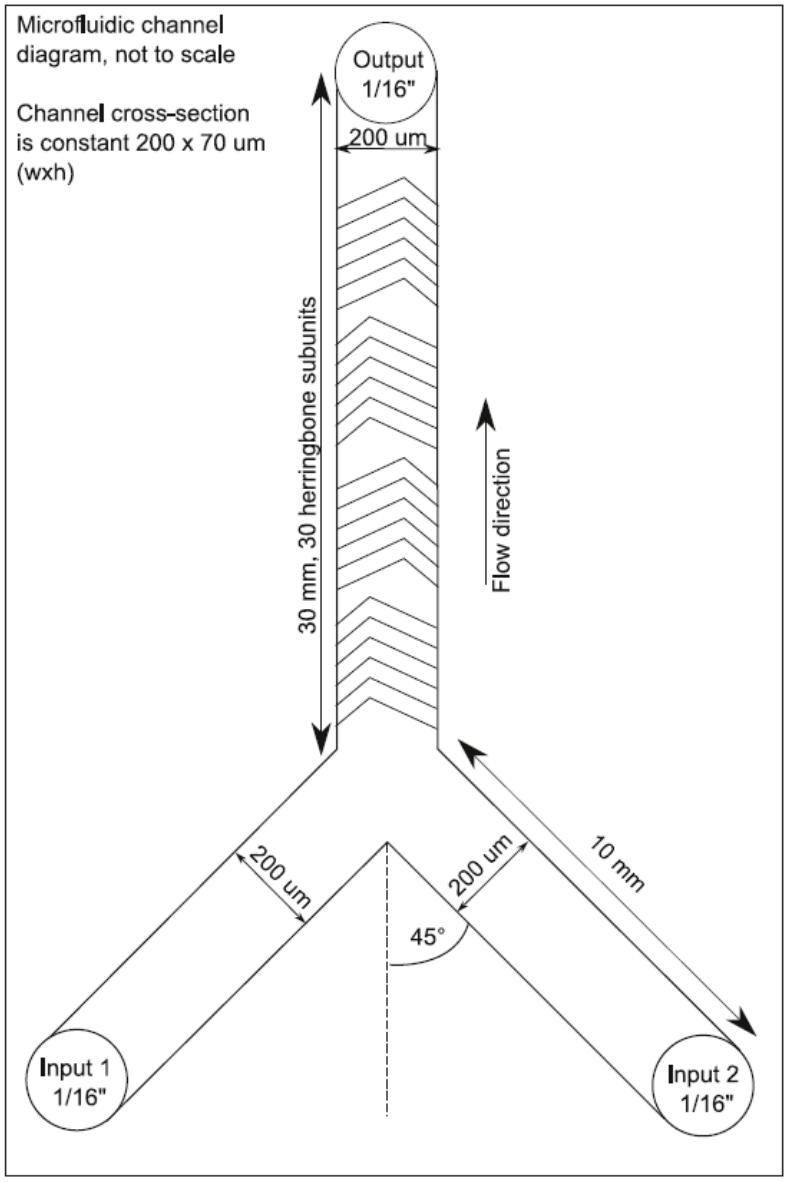

Fig. 18. **Scheme of the microfluidic device for LNPs assembly (uFluidix)**. The device contains two input channels for the solution of lipids and for mRNA. Output channel for solutions mixing is designed with special grooves for rapid mixing and formation of smaller nanoparticles (design was done by Jan Vávra and Dr. Petr Cígler).

5.1.5. Cell transfection with lipid nanoparticles

Lipid nanoparticles were further applied to different cell lines (HEK293T, Huh7, U2-OS, and CEM). Since the LNPs contained mRNA encoding fluorescent protein mKate2, it was possible to detect the efficiency of transfection and mRNA translation into the protein by measuring mKate2 fluorescence on the flow cytometer (Fig. 19). The cells were incubated with LNPs for 20 hours and the medium with LNPs was washed prior to cytometer

measurement. All cells from the well were measured, cell populations were selected and average values were generated using BD FACS Diva software programme.

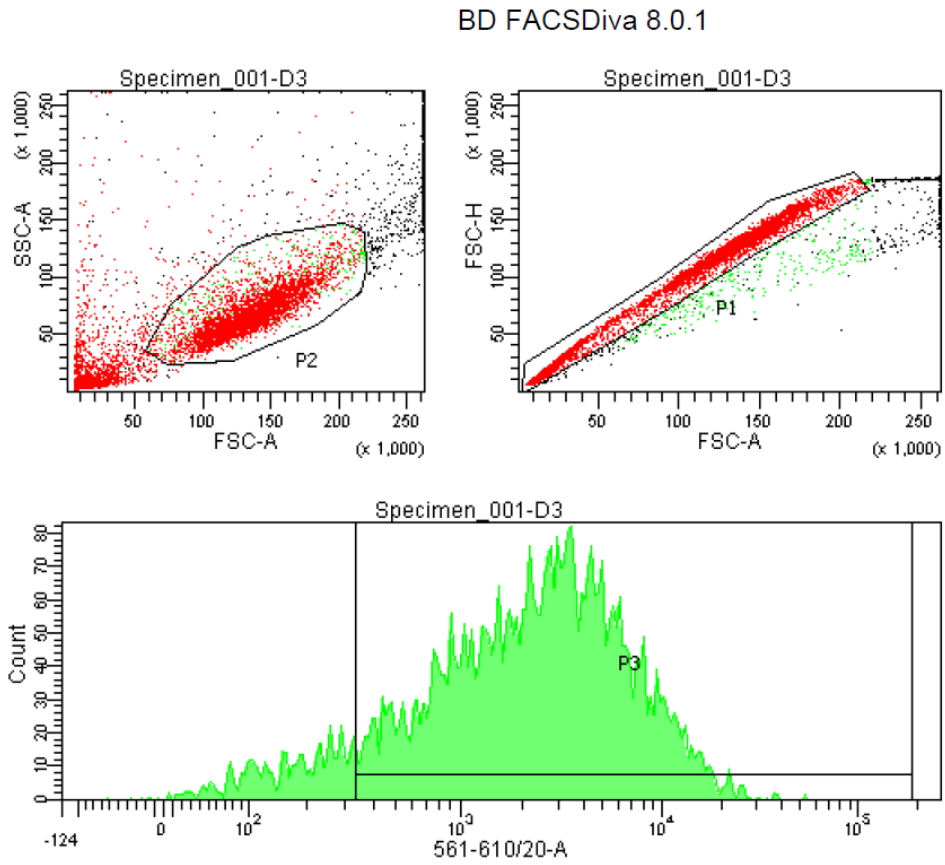

Fig. 19. **Flow cytometry of HEK293T cells transfected by LNPs with mKate2 mRNA.** The upper left scheme shows selected gate of the live cell population, upper right scheme shows selected gate of single cells. The signal of mKate2 fluorescence of the gated population is shown in the lower part.

The proper amount of mRNA used for LNPs assembly is not specified in the literature so the estimated amount of 120 µg was used for the experiments. Since the preparation of mRNA is quite expensive and time-consuming, the down-scale experiment was performed by using different amounts of mRNA for LNPs. All nanoparticles were further transfected to cells in 96-well plate and evaluated by flow cytometry (Table 4). The analysis suggests that there is a similar number of assembled nanoparticles with similar average diameters from all samples, however, a number of mRNA molecules inside one nanoparticle is different. Reduction of mRNA from 120 µg to 90 µg did not decrease the efficiency of transfection. Lower amounts were also efficient, but the decrease was more significant.

Table 4: **Transfection efficiency of LNPs with different amounts of mRNA evaluated via flow cytometry.** The table shows proportion of cells in 96-well plates positive for transfection and translation of mKate2 with mean and median values of the fluorescence for LNPs with 120, 90, 60 and 40 µg of mKate2 mRNA.

	mKate2 Fluorescence				
Sample	***%parents***	***mean***	***median***	**mRNA/LNPs**	**mRNA/well**
negative control	1,6	366	175	-	-
LNPs-120	99,9	15537	11869	120ug	200ng
LNPs-90	99,9	13814	10434	90ug	150ng
LNPs-60	99,9	8907	6747	60ug	100ng
LNPs-40	99,6	6219	4623	40ug	66ng

5.1.6. Evaluation of LNP stability

LNPs with mRNA were stored in the refrigerator after assembly for up to 6 weeks. They were usually applied to cells immediately after assembly, but to analyze their stability they were also transfected into the cells repeatedly every week. LNPs can transfect the cells with almost the same efficiency 2 weeks after the assembly, later the LNPs are still functional but the efficiency is slightly decreased.

Furthermore, it was shown that nanoparticles protect RNA cargo against degradation by nucleases. RNA of mKate2 was incubated for five minutes with different concentrations of RNase A to find the lowest concentration which still digests the RNA. We did not want to apply too big excess of RNAse since it could cause artificial results in cleavage or later in transfection of the cells. RNA samples were then applied to PAGE immediately to analyze the results. LNPs with encapsulated RNA were then incubated with RNase A of particular concentration for 3 hours and then transfected to the cells. After 20 hours, cells were measured on flow cytometer as usual for mKate2 fluorescence (Table 5). The fluorescence did not change in comparison with the original sample.

Table 5: **Transfection efficiency of LNPs after RNase treatment evaluated via flow cytometry.** Incubation of LNPs with RNase does not influence the efficiency of transfection and translation of mRNA cargo. Lipid nanoparticles reliably protect RNA against RNase degradation.

	Fluorescence of mKate2		
	% of positive cells	Mean	Median
Negative control	0	1855	874
Positive control	43	25772	9720
LNP sample	95	24475	16928
LNP sample after RNase treatment	96	19109	14053

5.1.7. Targeting cells via transferrin receptor

For potential application of LNPs with CRISPR/Cas9, it is necessary to deliver the cargo only to specific cells. As a model system, transferrin receptor was chosen as it was previously used in the laboratory of Dr. Cígler. Transferrin (Tf) was added to the surface of the nanoparticles after their assembly via click reaction. Transferrin was synthesized with *trans*-cyclooctene tag and DMG-PEG lipid was modified with tetrazine (Fig. 20). For targeting experiments, DMG-PEG-tetrazine was used in lipid mixture for LNPs assembly instead of original DMG-PEG.

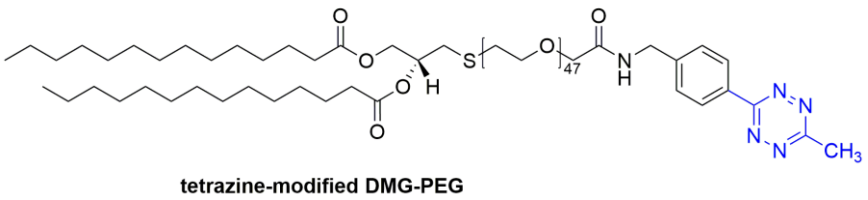

tetrazine-modified DMG-PEG

Fig. 20. **DMG-PEG lipid modified with tetrazine tag** (shown in blue) to enable the addition of transferrin or another targeting molecule with *trans*-cyclooctene tag.

LNPs obtained from the microfluidic device were mixed with 0,3 mg of modified Tf-*trans*-cyclooctene. The reaction should be fast, but in order to achieve the best results, it was incubated overnight. If the reaction was applied to cells immediately, free transferrin would bind to the transferrin receptors and it would block the transfection of the LNPs. Therefore, LNPs need to be purified from free transferrin. After numerous optimization, Sepharose 4B

column was chosen and prepared for purification. Elution fractions of 0.5 ml were collected from the column after application of LNPs-transferrin mixture (fractions were marked with letters, tags of fractions differ between individual experiments). Fractions were further analyzed by spectrophotometry (Fig. 21) to reveal which of them contain most nanoparticles. To visualize LNPs with clicked transferrin, absorbance was measured at 280 nm, which should correspond to protein levels (transferrin), however, it was shown that lipids also absorb at this wavelength so all LNPs are probably encaptured no matter if they contain transferrin or not. Moreover, fractions with LNPs were measured on DLS instrument to analyze their relative count rate. It was shown that relative count rate from DLS correlates to the transfection efficiency of particular LNP sample (Fig. 22).

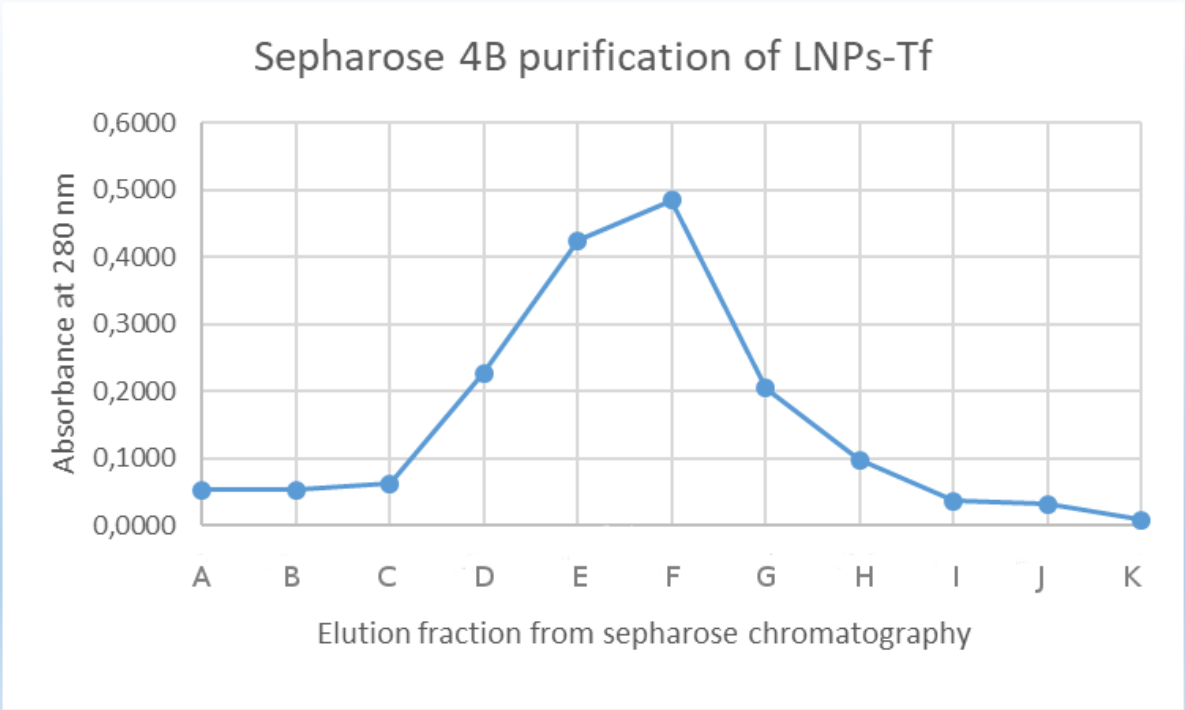

Fig. 21. **Detection of purified LNPs-Tf in fractions from Sepharose 4B column.** Nanoparticles were detected by measuring the absorbance of 280 nm which should be suitable for protein detection (transferrin).

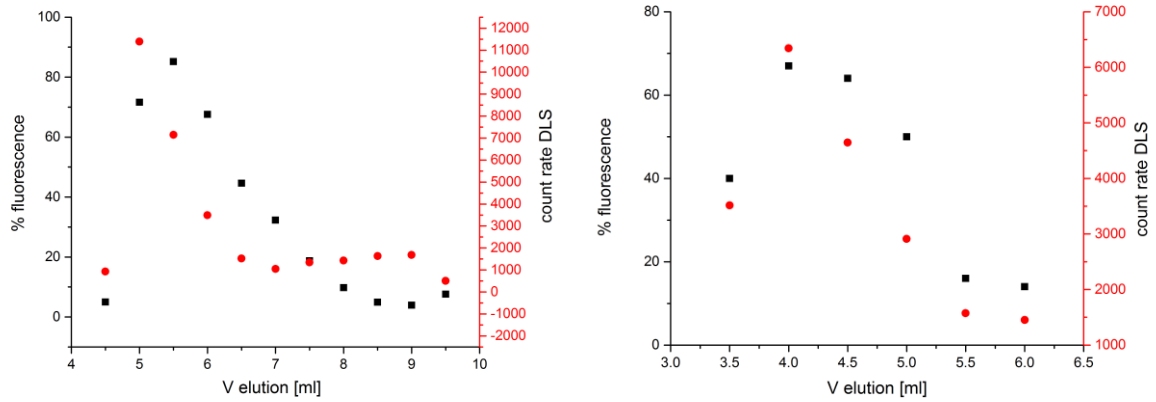

Fig. 22. **Correlation of LNP count rate and their transfection efficiency**. Results of elution fractions from Sepharose 4B column are plotted. Black dots represent the percentage of positive cells for mKate2 fluorescence after LNPs transfection obtained from flow cytometry measurement. Red dots show relative count rate of LNP sample determined by DLS measurement. The result of two different experiments is shown.

Furthermore, Tf-tetrazine was linked with Alexa488 fluorescent dye. LNPs were synthesized again, Tf was clicked and unbound Tf was washed away on the Sepharose 4B column as described above. Fractions with the highest number of particles were transfected into the U2-OS cells. Similar to the previous experiment, cells were analyzed by flow cytometry measuring mKate2 fluorescence (indicating delivery and translation of mRNA), plus fluorescence of Alexa488 (Table 6). These experiments enabled direct comparison of how many cells accepted the nanoparticles and how many of them also translated the mRNA into the protein. Overall, more than half of the cells transfected with LNP-Tf usually translate the fluorescent protein mKate2 (Fig.23).

Table 6: **Transfection of Huh7 cells with LNPs-Tf-alexa488 carrying mRNA of mKate2.** As a mock experiment, cells without LNPs were prepared. LNPs without transferrin showed 9-fold higher mKate2 fluorescence in comparison to negative control, with no increase in Alexa488 fluorescence. After transfection of nanoparticles coated with transferrin (best fraction from sepharose column – fraction A), 45 % of cells are positive for Alexa488 fluorescence, but only slight increase of fluorescence was observed compared to control. That could be caused by a low number of molecules clicked onto LNPs surface. Fluorescence of translated mKate2 is significantly higher from LNPs.

Huh7	Fluorescence of mKate2			Fluorescence of Alexa488		
Sample	**%parents**	**Mean**	**Median**	**%parents**	**Mean**	**Median**
control	1	296	283	0	434	399
LNPs	48	2637	1202	4	454	427
A	26	851	468	45	978	630
B	25	875	475	36	794	542

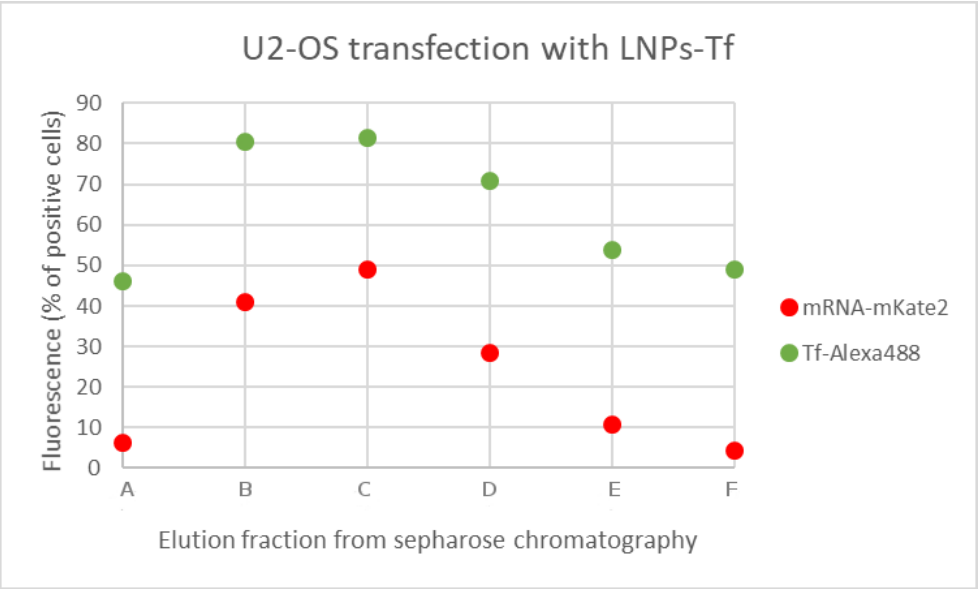

Fig. 23. **U2-OS cells transfected with LNP-Tf-Alexa488-mRNA encoding mKate2.** Elution fractions from Sepharose 4B column are plotted according to the percentage of positive cells from flow cytometry. The graph shows the fluorescence of Alexa488 representing nanoparticle entry and the fluorescence of mKate2 representing the successful translation of mRNA cargo.

In order to visualize unmodified LNPs and compare them directly to modified LNPs by Tf, DOPE lipid used for LNPs assembly was modified with fluorescent Cy5 tag. LNPs were synthesized as described above including transferrin-Alexa488 added by click reaction. However, Tf was not attached to the nanoparticles, which was obvious after the sepharose purification of LNPs, as it appeared to be in later fractions than usual (Fig. 24). Transferrin was found in fractions after 5.5 ml elution, while LNPs were in fractions of 0.5–3 ml. The quality analysis of the transferrin by thin-layer chromatography (done by Dr. Václav Vaněk, IOCB Prague) revealed that transferrin tag isomerized from its reactive *trans*-cyclooctene into a *cis*-cyclooctene conformation which is not reactive in click chemistry. For further experiments, it was thus necessary to synthesize new transferrin with active *trans*-cyclooctene moiety.

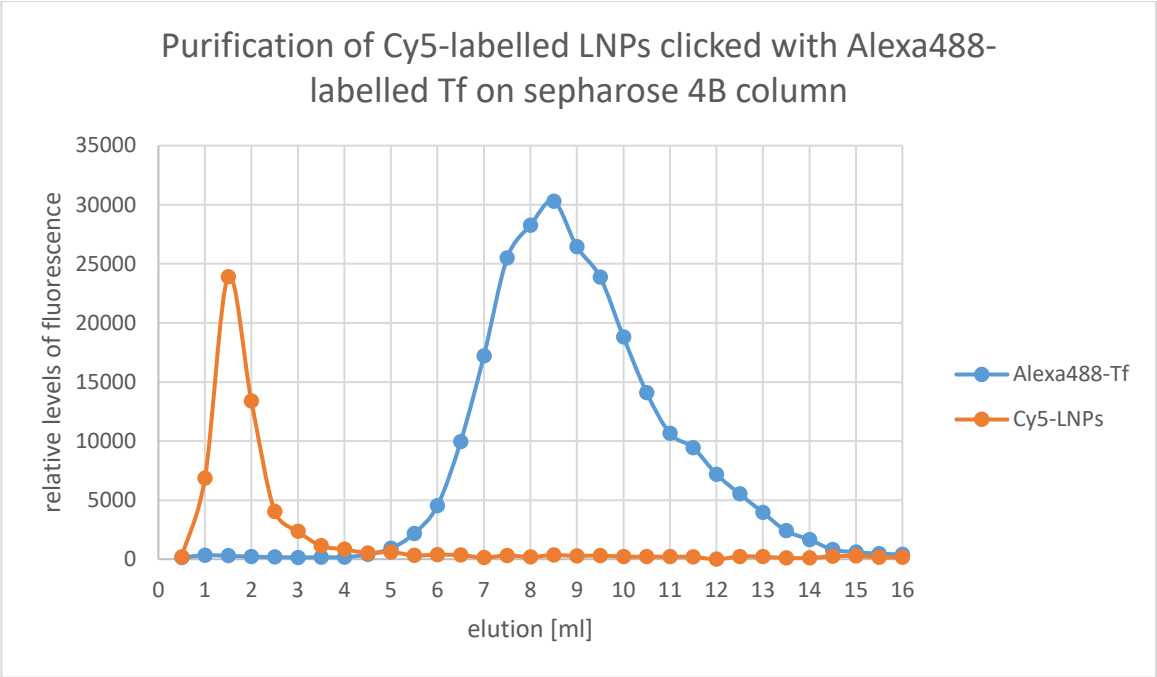

Fig. 24. **Sepharose 4B purification of LNPs from unbound transferrin.** LNPs were visualized by measuring the Cy5 fluorescence, transferrin accordingly by measuring the Alexa488 signal. Both substances were in different elution fractions indicating that transferrin was not attached to the LNPs by the click chemistry reaction.

5.1.8. Comparison of LNPs transfection efficiency in different cell lines

Three different cell lines (CEM, U2-OS, Huh7) were transfected with LNPs with clicked transferrin-Alexa488 and containing mRNA encoding mKate2 to evaluate its efficiency in different cell models (Fig. 25). CEM is a suspension cell line that is normally resistant to transfection by typical transfection reagents. CEM express transferrin receptor in relatively high levels thus this cell line represents almost ideal control of our targeted delivery system. Flow cytometry analysis revealed that about half of the cells are positive for Alexa488 (attached to the clicked transferrin), however, no mKate2 fluorescence was observed. Huh7 cells, on the other hand, can be transfected by standard methods, but the efficiency is quite low. Their transfection with our LNPs showed similar results. Interestingly, targeted delivery of our LNPs to U2-OS showed more promising results. The detailed mechanism still remains to be evaluated.

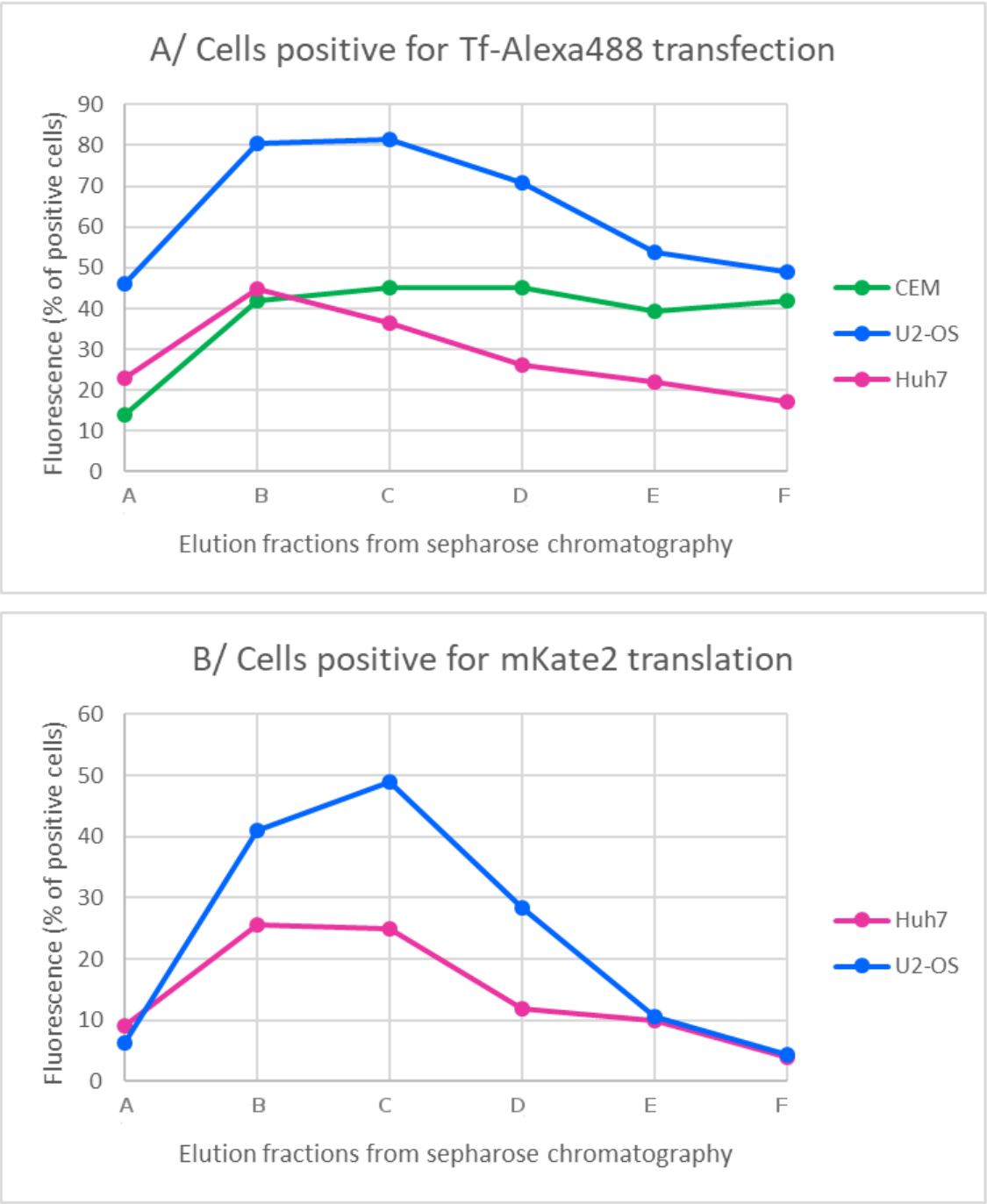

Fig. 25. Comparison of LNPs-Tf targeted delivery to three different cell lines. U2-OS, Huh7 and CEM cells were transfected with LNP-Tf-Alexa488 containing mKate2 mRNA. **A** Alexa488 fluorescence was observed in all three cell lines, transfection is most effective in case of U2-OS cells. **B** CEM cells do not translate any mRNA, U2-OS transfection is more efficient than Huh7.

6. Discussion

Current medical treatment of hepatitis B viral chronic infection is still not ideal since the viral cccDNA pool remains unaffected in the infected cells. The concept of disruption of HBV genome by CRISPR/Cas9 or other gene editing tools has been already proposed by several groups. All published sgRNAs targeted different regions within the HBV genome and showed different efficacies. In order to test some of the published data in our hands, three different published and characterized sgRNAs targeting HBV cccDNA were ordered and examined (data not shown). Surprisingly, we did not obtain the same results, but the overall trend of all three sgRNAs affecting cccDNA was comparable to the published literature. That assured us that the system works in our hands and that we could proceed to the design of our own guides.

CRISPR/Cas9 system has been extensively studied and used for various purposes in the past few years. Plasmid vectors with single or multiple guide scaffolds are relatively easy to get and they are provided with fast, easy and efficient cloning protocol. Online tools help to generate and evaluate appropriate guide sequences, so it is relatively simple to make your own CRISPR systems for the target of interest. In order to effectively cleave and possibly even degrade HBV cccDNA, we designed twelve sgRNAs targeting various regions within the HBV genome. Generally, we chose sequences within well conserved and stable regions, in order to affect most of the viral genotypes. Secondly, those regions are all assumed to be transcriptionally active since they encode viral structural proteins. An important aspect of an appropriate guide choice is its calculated probability of off-targets within the human genome. Therefore, only those guides with minimal predicted off-target activity were selected.

All of the guides were cloned into the dual expression vector pX333, enabling simultaneous expression of two sgRNAs and a Cas9 nuclease. The sgRNAs combination was chosen almost randomly with the only criteria that the length between the two cleavage sites should be bigger than 300bp.

Next, we set up initial experiments to evaluate the efficacies of our CRISPR/Cas9 system. All experiments were performed in the biosafety level 3 laboratory at IOCB, Prague. We used recombinant cccDNA transfected into the Huh7 cells, as discussed above, in order to work with a robust system since the viral infection in HepG2 cells (or HepG2-NTCP) is usually very inefficient. Therefore, rcccDNA and pX333 plasmids were co-transfected into the Huh7 cells and the efficacy of the cleavage was analyzed by detection of viral HBsAg and HBeAg antigens by commercial ELISA kit, six and twelve days post infection. Genes

encoding viral proteins such as polymerase, surface, core and protein X were targeted for the cleavage in dual combinations. Surface protein is usually not detectable six days post infection since its levels are below the detection limit of available ELISA kit. The co-transfection experiment with plasmids encoding dual sgRNAs was repeated in technical triplicate and biological duplicate. The results clearly show the overall significant decrease in viral antigens production. If the whole cccDNA molecule was after the double cleavage affected by severe mutagenesis or if it was even degraded still has to be analyzed by real-time PCR.

As a next logical step, we switched from DNA encoding CRISPR/Cas9 to RNA encoding Cas9 nuclease and individual sgRNAs. From the initial number of 12 guide sequences, those with the most promising results will be selected for further RNA experiments. Gene encoding Cas9 nuclease was cloned under T7 promoter into the expression vector and was subsequently *in vitro* transcribed in several reactions that were pooled together. The assembly of nanoparticles containing mRNA encoding Cas9 together with sgRNA is undergoing and it is not part of this thesis.

In order to effectively develop and characterize our LNPs, mRNA encoding fluorescent protein mKate2 was used instead of mRNA encoding Cas9 nuclease. Lipid nanoparticles harboring mRNA can be theoretically assembled by simple mixing similar to pipetting in an Eppendorf tube, however, the quality of such sample would be for our purpose unsatisfactory. Instead, more complexed methods were developed by others to increase the yield of small monodisperse lipid nanoparticles. Inspired by some of the published devices, we also developed in collaboration with Dr. Cígler group and IOCB workshop our own microfluidic device. Initially, the working solutions were mixed from the syringes by a mechanical push which resulted in a number of disadvantages. The flow rate and pressure inside the device could not be controlled, both syringes could not be simultaneously pressed at the exactly same time and they could not be pressed completely as the pressure was too high. Therefore, a new microfluidic device was ordered from the uFluidix company that was designed according to our instructions. This device enabled its connection to automatic pump and adjustment of stable flow rate which resulted in better quality of the nanoparticles.

The composition of lipid nanoparticles used in this study was inspired by the work of established lab in this field and it was the following: cholesterol, DOPE, TT3 lipid and DMG-PEG (4:3:2:1 ratio) and mRNA encoding mKate2 as described in chapter 3.3.2. Our significant addition to that composition is tetrazine-modified DMG-PEG enabling click reaction for attachment of the targeting moiety. LNPs were optimized and characterized by

measuring their diameter and zeta potential by DLS and visualized by TEM. The nanoparticles were about 150 nm in average size and relatively homogenous. Their transfection efficacy was always monitored by flow cytometry by measuring fluorescence of the translated mKate2 protein, and they were reasonably good in HEK293T, U2-OS and possibly Huh7 cells. LNPs proved stable in time (minimal up to 2 weeks) and they efficiently protect RNA cargo from RNase degradation.

Next, we selected a model "targeting" system based on transferrin and transferrin-receptor mediated endocytosis. LNPs were prepared by a microfluidic device with high yields and transferrin modified with trans-cyclooctene was then attached by click reaction onto the surface of already assembled nanoparticles. The click reaction by itself was very fast and efficient. *Trans*-cyclooctene is, however, very unstable reactive group and it is likely to undergo conversion to its *cis* isomer. *Cis*-cyclooctene does not react with the tetrazine so the molecule with conversed *cis*-cyclooctene is not linked to the nanoparticles. Therefore, targeting molecules with *trans*-cyclooctene cannot be prepared in higher quantities in advance, which makes the experiment more difficult and time-consuming.

LNPs coated with transferrin were tested with four different cell lines – HEK293T, U2-OS, Huh7, and CEM. These lipid nanoparticles are very efficient in mRNA delivery to cell lines like HEK293T and U2-OS and they bring a benefit for cell lines such as Huh7 which are normally transfected with low efficiencies. CEM cells were not successfully transfected even after the addition of transferrin. Flow cytometry analysis revealed that most of the CEM cells are positive for Alexa488 after transfection of LNP-Tf-Alexa488 with mKate2 mRNA, however, there is no mKate2 fluorescence detectable. This suggests that nanoparticles with transferrin were internalized but the mRNA was not translated. This could be due to a slightly different endosomal pathway of the CEM cells. In other cell lines, lower fluorescence was observed after LNPs-Tf delivery than in case of original nanoparticles without the targeting moiety. It could be caused by the smaller amount of LNPs-Tf used for the experiments. Another possible explanation is that the molecule of transferrin covers up the surface of the nanoparticle and blocks random internalization of lipid nanoparticles as they cannot interfere with the cell membrane. Further experiments in the near future will be done to uncover the true reason for that.

In summary, we have developed modular lipid nanoparticles harboring mRNA that are protecting its mRNA cargo from RNases and effectively delivering it into several human cell lines including hepatocytes. Further, we have designed twelve sgRNAs targeting HBV

cccDNA and effectively suppressing viral production. Next, we will combine both systems together in order to efficiently target HBV infected hepatocytes.

7. Conclusion

- Twelve different sgRNAs targeting HBV cccDNA were designed and cloned in dual combinations into the pX333 vector encoding Cas9 nuclease.

- HBV cccDNA was successfully cleaved by designed CRISPR/Cas9 system and viral production was thus effectively suppressed.

- Functional modular lipid nanoparticles with mRNA cargo were developed and tested for their targeted delivery through transferrin receptor.

- Lipid nanoparticles described in this thesis are very efficient in cell delivery. LNPs carried mRNA encoding fluorescent protein mKate2 so the transfection efficiency could be observed as mKate2 fluorescence which represented internalization of nanoparticles and translation of stable mRNA.

- Transferrin as a model targeting moiety was attached to the nanoparticles surface via click chemistry reaction. Transferrin was tagged with fluorescent Alexa488 for visualization and further analysis of transfection efficiencies.

- Both projects will be combined together. Lipid nanoparticles will be further assembled with CRISPR/Cas9 system encoded by RNA and tested for their ability to suppress or clear the HBV infection.

8. References

Anwer, M. S., & Stieger, B. (2014). Sodium-dependent bile salt transporters of the SLC10A transporter family: more than solute transporters. *Pflugers Arch, 466*(1), 77-89. doi:10.1007/s00424-013-1367-0

Barrangou, R., Fremaux, C., Deveau, H., Richards, M., Boyaval, P., Moineau, S., . . . Horvath, P. (2007). CRISPR provides acquired resistance against viruses in prokaryotes. *Science, 315*(5819), 1709-1712.

Beck, J., & Nassal, M. (2007). Hepatitis B virus replication. *World J Gastroenterol, 13*(1), 48-64.

Belloni, L., Pollicino, T., De Nicola, F., Guerrieri, F., Raffa, G., Fanciulli, M., . . . Levrero, M. (2009). Nuclear HBx binds the HBV minichromosome and modifies the epigenetic regulation of cccDNA function. *Proc Natl Acad Sci U S A, 106*(47), 19975-19979. doi:10.1073/pnas.0908365106

Bill, C. A., & Summers, J. (2004). Genomic DNA double-strand breaks are targets for hepadnaviral DNA integration. *Proc Natl Acad Sci U S A, 101*(30), 11135-11140. doi:10.1073/pnas.0403925101

Bock, C. T., Schwinn, S., Locarnini, S., Fyfe, J., Manns, M. P., Trautwein, C., & Zentgraf, H. (2001). Structural organization of the hepatitis B virus minichromosome. *J Mol Biol, 307*(1), 183-196. doi:10.1006/jmbi.2000.4481

Boch, J., Scholze, H., Schornack, S., Landgraf, A., Hahn, S., Kay, S., . . . Bonas, U. (2009). Breaking the Code of DNA Binding Specificity of TAL-Type III Effectors. *Science, 326*(5959), 1509-1512.

Cong, L., Ran, F. A., Cox, D., Lin, S., Barretto, R., Habib, N., . . . Zhang, F. (2013). Multiplex genome engineering using CRISPR/Cas systems. *Science, 339*(6121), 819-823. doi:10.1126/science.1231143

Dandri, M., Burda, M. R., Will, H., & Petersen, J. (2000). Increased hepatocyte turnover and inhibition of woodchuck hepatitis B virus replication by adefovir in vitro do not lead to reduction of the closed circular DNA. *Hepatology, 32*(1), 139-146. doi:10.1053/jhep.2000.8701

Deltcheva, E., Chylinski, K., Sharma, C. M., Gonzales, K., Chao, Y. J., Pirzada, Z. A., . . . Charpentier, E. (2011). CRISPR RNA maturation by trans-encoded small RNA and host factor RNase III. *Nature, 471*(7340), 602-+.

Dong, C., Qu, L., Wang, H., Wei, L., Dong, Y., & Xiong, S. (2015). Targeting hepatitis B virus cccDNA by CRISPR/Cas9 nuclease efficiently inhibits viral replication. *Antiviral Res, 118*, 110-117. doi:10.1016/j.antiviral.2015.03.015

Dupinay, T., Gheit, T., Roques, P., Cova, L., Chevallier-Queyron, P., Tasahsu, S. I., . . . Chemin, I. (2013). Discovery of naturally occurring transmissible chronic hepatitis B virus infection among Macaca fascicularis from Mauritius Island. *Hepatology, 58*(5), 1610-1620. doi:10.1002/hep.26428

Durantel, D., & Zoulim, F. (2016). New antiviral targets for innovative treatment concepts for hepatitis B virus and hepatitis delta virus. *J Hepatol, 64*(1 Suppl), S117-S131. doi:10.1016/j.jhep.2016.02.016

Evans, D. T., Serra-Moreno, R., Singh, R. K., & Guatelli, J. C. (2010). BST-2/tetherin: a new component of the innate immune response to enveloped viruses. *Trends Microbiol, 18*(9), 388-396. doi:10.1016/j.tim.2010.06.010

Friedland, A. E., Baral, R., Singhal, P., Loveluck, K., Shen, S., Sanchez, M., . . . Bumcrot, D. (2015). Characterization of Staphylococcus aureus Cas9: a smaller Cas9 for all-in-one adeno-associated virus delivery and paired nickase applications. *Genome Biol, 16*, 257. doi:10.1186/s13059-015-0817-8

Gasiunas, G., Barrangou, R., Horvath, P., & Siksnys, V. (2012). Cas9-crRNA ribonucleoprotein complex mediates specific DNA cleavage for adaptive immunity in bacteria. *Proc Natl Acad Sci U S A, 109*(39), E2579-2586. doi:10.1073/pnas.1208507109

Grimm, D., Thimme, R., & Blum, H. E. (2011). HBV life cycle and novel drug targets. *Hepatol Int, 5*(2), 644-653. doi:10.1007/s12072-011-9261-3

Guo, X., Chen, P., Hou, X., Xu, W., Wang, D., Wang, T. Y., . . . Chen, Z. Y. (2016). The recombined cccDNA produced using minicircle technology mimicked HBV genome in structure and function closely. *Sci Rep, 6*, 25552. doi:10.1038/srep25552

Gupta, R. M., & Musunuru, K. (2014). Expanding the genetic editing tool kit: ZFNs, TALENs, and CRISPR-Cas9. *Journal of Clinical Investigation, 124*(10), 4154-4161.

Guy, C. S., Mulrooney-Cousins, P. M., Churchill, N. D., & Michalak, T. I. (2008). Intrahepatic expression of genes affiliated with innate and adaptive immune responses immediately after invasion and during acute infection with woodchuck hepadnavirus. *J Virol, 82*(17), 8579-8591. doi:10.1128/JVI.01022-08

Heyes, J., Hall, K., Tailor, V., Lenz, R., & MacLachlan, I. (2006). Synthesis and characterization of novel poly(ethylene glycol)-lipid conjugates suitable for use in drug delivery. *J Control Release, 112*(2), 280-290. doi:10.1016/j.jconrel.2006.02.012

Hirsch-Lerner, D., Zhang, M., Eliyahu, H., Ferrari, M. E., Wheeler, C. J., & Barenholz, Y. (2005). Effect of "helper lipid" on lipoplex electrostatics. *Biochim Biophys Acta, 1714*(2), 71-84. doi:10.1016/j.bbamem.2005.04.008

Huang, J. Y., Chou, S. F., Lee, J. W., Chen, H. L., Chen, C. M., Tao, M. H., & Shih, C. (2015). MicroRNA-130a can inhibit hepatitis B virus replication via targeting PGC1alpha and PPARgamma. *RNA, 21*(3), 385-400. doi:10.1261/rna.048744.114

Hurley, J. H. (2015). ESCRTs are everywhere. *EMBO J, 34*(19), 2398-2407. doi:10.15252/embj.201592484

Chen, C. J., & Yang, H. I. (2011). Natural history of chronic hepatitis B REVEALed. *J Gastroenterol Hepatol, 26*(4), 628-638. doi:10.1111/j.1440-1746.2011.06695.x

Chen, D., Love, K. T., Chen, Y., Eltoukhy, A. A., Kastrup, C., Sahay, G., . . . Anderson, D. G. (2012). Rapid discovery of potent siRNA-containing lipid nanoparticles enabled by controlled microfluidic formulation. *J Am Chem Soc, 134*(16), 6948-6951. doi:10.1021/ja301621z

Ishino, Y., Shinagawa, H., Makino, K., Amemura, M., & Nakata, A. (1987). Nucleotide-Sequence of the Iap Gene, Responsible for Alkaline-Phosphatase Isozyme Conversion in Escherichia-Coli, and Identification of the Gene-Product. *Journal of Bacteriology, 169*(12), 5429-5433.

Jemielity, J., Fowler, T., Zuberek, J., Stepinski, J., Lewdorowicz, M., Niedzwiecka, A., . . . Rhoads, R. E. (2003). Novel "anti-reverse" cap analogs with superior translational properties. *RNA, 9*(9), 1108-1122.

Jinek, M., Chylinski, K., Fonfara, I., Hauer, M., Doudna, J. A., & Charpentier, E. (2012). A programmable dual-RNA-guided DNA endonuclease in adaptive bacterial immunity. *Science, 337*(6096), 816-821. doi:10.1126/science.1225829

Kaneko, M., Futamura, Y., Tsukuda, S., Kondoh, Y., Sekine, T., Hirano, H., . . . Watashi, K. (2018). Chemical array system, a platform to identify novel hepatitis B virus entry inhibitors targeting sodium taurocholate cotransporting polypeptide. *Sci Rep, 8*(1), 2769. doi:10.1038/s41598-018-20987-w

Kennedy, E. M., Bassit, L. C., Mueller, H., Kornepati, A. V., Bogerd, H. P., Nie, T., . . . Cullen, B. R. (2015). Suppression of hepatitis B virus DNA accumulation in chronically infected cells using a bacterial CRISPR/Cas RNA-guided DNA endonuclease. *Virology, 476*, 196-205. doi:10.1016/j.virol.2014.12.001

Kersseboom, S., van Gucht, A. L. M., van Mullem, A., Brigante, G., Farina, S., Carlsson, B., . . . Visser, T. J. (2017). Role of the Bile Acid Transporter SLC10A1 in Liver Targeting of the Lipid-Lowering Thyroid Hormone Analog Eprotirome. *Endocrinology, 158*(10), 3307-3318. doi:10.1210/en.2017-00433

Lau, J. Y., & Wright, T. L. (1993). Molecular virology and pathogenesis of hepatitis B. *Lancet, 342*(8883), 1335-1340.

Lepenies, B., Lee, J., & Sonkaria, S. (2013). Targeting C-type lectin receptors with multivalent carbohydrate ligands. *Adv Drug Deliv Rev, 65*(9), 1271-1281. doi:10.1016/j.addr.2013.05.007

Li, B., Luo, X., Deng, B., Wang, J., McComb, D. W., Shi, Y., . . . Dong, Y. (2015). An Orthogonal Array Optimization of Lipid-like Nanoparticles for mRNA Delivery in Vivo. *Nano Lett, 15*(12), 8099-8107. doi:10.1021/acs.nanolett.5b03528

Li, H., Sheng, C., Liu, H., Liu, G., Du, X., Du, J., . . . Song, H. (2016). An Effective Molecular Target Site in Hepatitis B Virus S Gene for Cas9 Cleavage and Mutational Inactivation. *Int J Biol Sci, 12*(9), 1104-1113. doi:10.7150/ijbs.16064

Lin, G., Zhang, K., & Li, J. (2015). Application of CRISPR/Cas9 Technology to HBV. *Int J Mol Sci, 16*(11), 26077-26086. doi:10.3390/ijms161125950

Lin, S. R., Yang, H. C., Kuo, Y. T., Liu, C. J., Yang, T. Y., Sung, K. C., . . . Chen, P. J. (2014). The CRISPR/Cas9 System Facilitates Clearance of the Intrahepatic HBV Templates In Vivo. *Mol Ther Nucleic Acids, 3*, e186. doi:10.1038/mtna.2014.38

Liu, C., Zhang, L., Liu, H., & Cheng, K. (2017). Delivery strategies of the CRISPR-Cas9 gene-editing system for therapeutic applications. *J Control Release, 266*, 17-26. doi:10.1016/j.jconrel.2017.09.012

Liu, F., Song, Y., & Liu, D. (1999). Hydrodynamics-based transfection in animals by systemic administration of plasmid DNA. *Gene Ther, 6*(7), 1258-1266. doi:10.1038/sj.gt.3300947

Liu, X., Hao, R., Chen, S., Guo, D., & Chen, Y. (2015). Inhibition of hepatitis B virus by the CRISPR/Cas9 system via targeting the conserved regions of the viral genome. *J Gen Virol, 96*(8), 2252-2261. doi:10.1099/vir.0.000159

Lucifora, J., Xia, Y., Reisinger, F., Zhang, K., Stadler, D., Cheng, X., . . . Protzer, U. (2014). Specific and nonhepatotoxic degradation of nuclear hepatitis B virus cccDNA. *Science, 343*(6176), 1221-1228. doi:10.1126/science.1243462

Luo, X., Li, B., Zhang, X., Zhao, W., Bratasz, A., Deng, B., . . . Dong, Y. (2017). Dual-functional lipid-like nanoparticles for delivery of mRNA and MRI contrast agents. *Nanoscale, 9*(4), 1575-1579. doi:10.1039/c6nr08496f

Maddalo, D., Manchado, E., Concepcion, C. P., Bonetti, C., Vidigal, J. A., Han, Y. C., . . . Ventura, A. (2014). In vivo engineering of oncogenic chromosomal rearrangements with the CRISPR/Cas9 system. *Nature, 516*(7531), 423-427. doi:10.1038/nature13902

Mali, P., Yang, L., Esvelt, K. M., Aach, J., Guell, M., DiCarlo, J. E., . . . Church, G. M. (2013). RNA-guided human genome engineering via Cas9. *Science, 339*(6121), 823-826. doi:10.1126/science.1232033

Malone, R. W., Felgner, P. L., & Verma, I. M. (1989). Cationic liposome-mediated RNA transfection. *Proc Natl Acad Sci U S A, 86*(16), 6077-6081.

Midoux, P., & Pichon, C. (2015). Lipid-based mRNA vaccine delivery systems. *Expert Rev Vaccines, 14*(2), 221-234. doi:10.1586/14760584.2015.986104

Mihaila, R., Chang, S., Wei, A. T., Hu, Z. Y., Ruhela, D., Shadel, T. R., . . . Mathre, D. J. (2011). Lipid nanoparticle purification by spin centrifugation-dialysis (SCD): a facile and high-throughput approach for small scale preparation of siRNA-lipid complexes. *Int J Pharm, 420*(1), 118-121. doi:10.1016/j.ijpharm.2011.08.017

Miller, J., Mclachlan, A. D., & Klug, A. (1985). Repetitive Zinc-Binding Domains in the Protein Transcription Factor Iiia from Xenopus Oocytes. *Embo Journal, 4*(6), 1609-1614.

Miller, J. B., Zhang, S., Kos, P., Xiong, H., Zhou, K., Perelman, S. S., . . . Siegwart, D. J. (2017). Non-Viral CRISPR/Cas Gene Editing In Vitro and In Vivo Enabled by Synthetic Nanoparticle Co-Delivery of Cas9 mRNA and sgRNA. *Angew Chem Int Ed Engl, 56*(4), 1059-1063. doi:10.1002/anie.201610209

Miller, J. C., Tan, S. Y., Qiao, G. J., Barlow, K. A., Wang, J. B., Xia, D. F., . . . Rebar, E. J. (2011). A TALE nuclease architecture for efficient genome editing. *Nature Biotechnology, 29*(2), 143-U149.

Niu, Y., Shen, B., Cui, Y., Chen, Y., Wang, J., Wang, L., . . . Sha, J. (2014). Generation of gene-modified cynomolgus monkey via Cas9/RNA-mediated gene targeting in one-cell embryos. *Cell, 156*(4), 836-843. doi:10.1016/j.cell.2014.01.027

Pathak, P. O., Nagarsenker, M. S., Barhate, C. R., Padhye, S. G., Dhawan, V. V., Bhattacharyya, D., . . . Fahr, A. (2015). Cholesterol anchored arabinogalactan for asialoglycoprotein receptor targeting: synthesis, characterization, and proof of concept of hepatospecific delivery. *Carbohydr Res, 408*, 33-43. doi:10.1016/j.carres.2015.03.003

Pattanayak, V., Ramirez, C. L., Joung, J. K., & Liu, D. R. (2011). Revealing off-target cleavage specificities of zinc-finger nucleases by in vitro selection. *Nature Methods, 8*(9), 765-U115.

Phua, K. K., Leong, K. W., & Nair, S. K. (2013). Transfection efficiency and transgene expression kinetics of mRNA delivered in naked and nanoparticle format. *J Control Release, 166*(3), 227-233. doi:10.1016/j.jconrel.2012.12.029

Ramanan, V., Shlomai, A., Cox, D. B., Schwartz, R. E., Michailidis, E., Bhatta, A., . . . Bhatia, S. N. (2015). CRISPR/Cas9 cleavage of viral DNA efficiently suppresses hepatitis B virus. *Sci Rep, 5*, 10833. doi:10.1038/srep10833

Sanhueza, C. A., Baksh, M. M., Thuma, B., Roy, M. D., Dutta, S., Preville, C., . . . Mascitti, V. (2017). Efficient Liver Targeting by Polyvalent Display of a Compact Ligand for the Asialoglycoprotein Receptor. *J Am Chem Soc, 139*(9), 3528-3536. doi:10.1021/jacs.6b12964

Santiago, Y., Chan, E., Liu, P. Q., Orlando, S., Zhang, L., Urnov, F. D., . . . Collingwood, T. N. (2008). Targeted gene knockout in mammalian cells by using engineered zinc-finger nucleases. *Proc Natl Acad Sci U S A, 105*(15), 5809-5814. doi:10.1073/pnas.0800940105

Sapranauskas, R., Gasiunas, G., Fremaux, C., Barrangou, R., Horvath, P., & Siksnys, V. (2011). The Streptococcus thermophilus CRISPR/Cas system provides immunity in Escherichia coli. *Nucleic Acids Res, 39*(21), 9275-9282. doi:10.1093/nar/gkr606

Seeger, C., & Mason, W. S. (2015). Molecular biology of hepatitis B virus infection. *Virology, 479-480*, 672-686. doi:10.1016/j.virol.2015.02.031

Seeger, C., & Sohn, J. A. (2014). Targeting Hepatitis B Virus With CRISPR/Cas9. *Mol Ther Nucleic Acids, 3*, e216. doi:10.1038/mtna.2014.68

Shih, C., Chou, S. F., Yang, C. C., Huang, J. Y., Choijilsuren, G., & Jhou, R. S. (2016). Control and Eradication Strategies of Hepatitis B Virus. *Trends Microbiol, 24*(9), 739-749. doi:10.1016/j.tim.2016.05.006

Schultz, U., Summers, J., Staeheli, P., & Chisari, F. V. (1999). Elimination of duck hepatitis B virus RNA-containing capsids in duck interferon-alpha-treated hepatocytes. *J Virol, 73*(7), 5459-5465.

Simsek, E., Lu, X., Ouzounov, S., Block, T. M., & Mehta, A. S. (2006). alpha-Glucosidase inhibitors have a prolonged antiviral effect against hepatitis B virus through the sustained inhibition of the large and middle envelope glycoproteins. *Antivir Chem Chemother, 17*(5), 259-267. doi:10.1177/095632020601700503

Sonoda, E., Hochegger, H., Saberi, A., Taniguchi, Y., & Takeda, S. (2006). Differential usage of non-homologous end-joining and homologous recombination in double strand break repair. *DNA Repair (Amst), 5*(9-10), 1021-1029. doi:10.1016/j.dnarep.2006.05.022

Summers, J., Jilbert, A. R., Yang, W., Aldrich, C. E., Saputelli, J., Litwin, S., . . . Mason, W. S. (2003). Hepatocyte turnover during resolution of a transient hepadnaviral infection. *Proc Natl Acad Sci U S A, 100*(20), 11652-11659. doi:10.1073/pnas.1635109100

Summers, J., O'Connell, A., & Millman, I. (1975). Genome of hepatitis B virus: restriction enzyme cleavage and structure of DNA extracted from Dane particles. *Proc Natl Acad Sci U S A, 72*(11), 4597-4601.

Sun, D., Rosler, C., Kidd-Ljunggren, K., & Nassal, M. (2010). Quantitative assessment of the antiviral potencies of 21 shRNA vectors targeting conserved, including structured, hepatitis B virus sites. *J Hepatol, 52*(6), 817-826. doi:10.1016/j.jhep.2009.10.038

Taylor, M. T., Blackman, M. L., Dmitrenko, O., & Fox, J. M. (2011). Design and synthesis of highly reactive dienophiles for the tetrazine-trans-cyclooctene ligation. *J Am Chem Soc, 133*(25), 9646-9649. doi:10.1021/ja201844c

Tropberger, P., Mercier, A., Robinson, M., Zhong, W., Ganem, D. E., & Holdorf, M. (2015). Mapping of histone modifications in episomal HBV cccDNA uncovers an unusual chromatin organization amenable to epigenetic manipulation. *Proc Natl Acad Sci U S A, 112*(42), E5715-5724. doi:10.1073/pnas.1518090112

Volz, T., Allweiss, L., Ben, M. M., Warlich, M., Lohse, A. W., Pollok, J. M., . . . Dandri, M. (2013). The entry inhibitor Myrcludex-B efficiently blocks intrahepatic virus spreading in humanized mice previously infected with hepatitis B virus. *J Hepatol, 58*(5), 861-867. doi:10.1016/j.jhep.2012.12.008

Wang, J., Xu, Z. W., Liu, S., Zhang, R. Y., Ding, S. L., Xie, X. M., . . . Lu, F. M. (2015). Dual gRNAs guided CRISPR/Cas9 system inhibits hepatitis B virus replication. *World J Gastroenterol, 21*(32), 9554-9565. doi:10.3748/wjg.v21.i32.9554

Warren, K. S., Heeney, J. L., Swan, R. A., Heriyanto, & Verschoor, E. J. (1999). A new group of hepadnaviruses naturally infecting orangutans (Pongo pygmaeus). *J Virol, 73*(9), 7860-7865.

Watashi, K., Sluder, A., Daito, T., Matsunaga, S., Ryo, A., Nagamori, S., . . . Wakita, T. (2014). Cyclosporin A and its analogs inhibit hepatitis B virus entry into cultured hepatocytes through targeting a membrane transporter, sodium taurocholate cotransporting polypeptide (NTCP). *Hepatology, 59*(5), 1726-1737. doi:10.1002/hep.26982

Wooddell, C. I., Rozema, D. B., Hossbach, M., John, M., Hamilton, H. L., Chu, Q., . . . Lewis, D. L. (2013). Hepatocyte-targeted RNAi therapeutics for the treatment of chronic hepatitis B virus infection. *Mol Ther, 21*(5), 973-985. doi:10.1038/mt.2013.31

Wynne, S. A., Crowther, R. A., & Leslie, A. G. (1999). The crystal structure of the human hepatitis B virus capsid. *Mol Cell, 3*(6), 771-780.

Yan, H., Peng, B., Liu, Y., Xu, G., He, W., Ren, B., . . . Li, W. (2014). Viral entry of hepatitis B and D viruses and bile salts transportation share common molecular determinants on sodium taurocholate cotransporting polypeptide. *J Virol, 88*(6), 3273-3284. doi:10.1128/JVI.03478-13

Yan, H., Zhong, G., Xu, G., He, W., Jing, Z., Gao, Z., . . . Li, W. (2012). Sodium taurocholate cotransporting polypeptide is a functional receptor for human hepatitis B and D virus. *Elife, 3*. doi:10.7554/eLife.00049

Yin, H., Kanasty, R. L., Eltoukhy, A. A., Vegas, A. J., Dorkin, J. R., & Anderson, D. G. (2014). Non-viral vectors for gene-based therapy. *Nat Rev Genet, 15*(8), 541-555. doi:10.1038/nrg3763

Yin, H., Song, C. Q., Dorkin, J. R., Zhu, L. J., Li, Y., Wu, Q., . . . Anderson, D. G. (2016). Therapeutic genome editing by combined viral and non-viral delivery of CRISPR system components in vivo. *Nat Biotechnol, 34*(3), 328-333. doi:10.1038/nbt.3471

Yin, H., Song, C. Q., Suresh, S., Wu, Q., Walsh, S., Rhym, L. H., . . . Anderson, D. G. (2017). Structure-guided chemical modification of guide RNA enables potent non-viral in vivo genome editing. *Nat Biotechnol, 35*(12), 1179-1187. doi:10.1038/nbt.4005

Zeisel, M. B., Lucifora, J., Mason, W. S., Sureau, C., Beck, J., Levrero, M., . . . Zoulim, F. (2015). Towards an HBV cure: state-of-the-art and unresolved questions--report of the ANRS workshop on HBV cure. *Gut, 64*(8), 1314-1326. doi:10.1136/gutjnl-2014-308943

Zhen, S., Hua, L., Liu, Y. H., Gao, L. C., Fu, J., Wan, D. Y., . . . Gao, X. (2015). Harnessing the clustered regularly interspaced short palindromic repeat (CRISPR)/CRISPR-associated Cas9 system to disrupt the hepatitis B virus. *Gene Ther, 22*(5), 404-412. doi:10.1038/gt.2015.2

Zohra, F. T., Maitani, Y., & Akaike, T. (2012). mRNA delivery through fibronectin associated liposome-apatite particles: a new approach for enhanced mRNA transfection to mammalian cell. *Biol Pharm Bull, 35*(1), 111-115.

Zuckerman, A. J., Thornton, A., Howard, C. R., Tsiquaye, K. N., Jones, D. M., & Brambell, M. R. (1978). Hepatitis B outbreak among chimpanzees at the London Zoo. *Lancet, 2*(8091), 652-654.

Zuris, J. A., Thompson, D. B., Shu, Y., Guilinger, J. P., Bessen, J. L., Hu, J. H., . . . Liu, D. R. (2015). Cationic lipid-mediated delivery of proteins enables efficient protein-based genome editing in vitro and in vivo. *Nat Biotechnol, 33*(1), 73-80. doi:10.1038/nbt.3081

WHO 2017: http://www.who.int/mediacentre/factsheets/fs204/en/

CRISPR/Cas9 design tool used in the study: http://crispr.mit.edu/

HBV database used in the study: https://hbvdb.ibcp.fr/HBVdb/HBVdbIndex